



An inventory of Norway's glaciers and ice-marginal lakes from 2018–19 Sentinel-2 data

Article

Liss M. Andreassen¹ , Teodor Nagy¹, Bjarne Kjøllmoen¹ and Joshua R. Leigh² 

Cite this article: Andreassen LM, Nagy T, Kjøllmoen B, Leigh JR (2022). An inventory of Norway's glaciers and ice-marginal lakes from 2018–19 Sentinel-2 data. *Journal of Glaciology* 68(272), 1085–1106. <https://doi.org/10.1017/jog.2022.20>

Received: 17 June 2021

Revised: 4 March 2022

Accepted: 4 March 2022

First published online: 31 March 2022

Keywords:

glacier; glacier lakes; ice-marginal lakes; orthophotos; Pléiades; satellite; Sentinel-2

Author for correspondence:

Liss M. Andreassen,
E-mail: lma@nve.no

¹Section for Glaciers, Ice and Snow, Norwegian Water Resources and Energy Directorate (NVE), Oslo, Norway and ²University of Durham, Durham, UK

Abstract

We used Sentinel-2 satellite imagery at 10 m resolution to map the extent of Norway's glaciers and ice-marginal lakes over 2018–19. We applied a standardized semi-automated band ratio method to derive glacier outlines and ice-marginal lakes. To optimise the results, we manually edited the ice-lake interfaces, debris, snow and parts of the glaciers situated under shadow. We compared our Sentinel-2 derived outlines with very high-resolution aerial orthophotos and Pléiades satellite orthoimages. Glaciers larger than 0.3 km² have area differences within 7%, whereas values are larger for smaller glaciers. The orthophotos and orthoimages provide more details and a higher mapping accuracy for individual glaciers, but require manual digitisation, have smaller spatial and temporal coverage and can have adverse snow conditions. We found a total glacier area of 2328 ± 70 km² of which the ten largest glaciers accounted for 52%. The glacier area decreased 15% since the previous inventory (Landsat data from 1999 to 2006), the reduction being largest in northern Norway (22%) compared to southern Norway (10%). We detected more than 2000 previously undetected smaller glaciers and ice patches (covering 37 km²) and 360 new ice-marginal lakes.

1. Introduction

Glacier outlines are used in a range of glaciological and hydrological applications. An accurate mask of ice on land is needed for glaciological and hydrological modelling and to have up to date information on the state of glaciers. Furthermore, repeated glacier inventories are required to assess changes in glacier area and length. Satellite data are well suited for regional glacier mapping using standardized semi-automated methods as the images cover large areas (e.g. Paul and others, 2009; Racoviteanu and others, 2009). Sensors such as Landsat TM (since 1984) and later Landsat versions, ASTER (since 2000) and Sentinel-2 (since 2015) are the backbone of global glacier inventories such as the Global Land Ice Measurements from Space (GLIMS) database (Raup and others, 2007; Paul and others, 2016) and the Randolph Glacier Inventory (RGI) (e.g. Pfeffer and others, 2014; RGI Consortium, 2017).

Glacier lakes, also called ice-marginal lakes or proglacial lakes, are lakes formed along the glacier margin where the land along the ice margin slopes towards the ice or when a lake is dammed by the ice or a moraine. As glaciers shrink, existing glacier lakes can expand, vanish or detach from the glacier, and new glacier lakes can form at the termini. Glacier lakes are growing worldwide (Shugar and others, 2020) and may have substantial sub-glacial and englacial reservoirs (Bigelow and others, 2020). Ice-dammed lakes can cause catastrophic glacier lake outburst floods (GLOFs) or jökulhlaups when these dams fail (e.g. Liestøl, 1956; Reynolds, 1999; Harrison and others, 2018; Veh and others, 2018; Zheng and others, 2021). Glacier thinning can also result in more frequent lake drainage events (Capps and Clague, 2014). Glacier termini calving into lakes cause enhanced melting (Carrivick and Tweed, 2013). Recent analysis of glacier recession in northern Norway revealed that since the little ice age maximum all glaciers with an area loss of >50% were fronted by proglacial lakes (Leigh and others, 2020). Proglacial lakes also impact downstream fluvial sediment transport and are thus important for hydropower production and river sedimentation (Bogen and others, 2014). Glacier lakes are mapped using optical imagery (e.g. Bolch and others, 2008; Zhang and others, 2018; Qayyum and others, 2020) or radar satellite imagery (Strozzi and others, 2012) or a combination (Wangchuk and Bolch, 2020; How and others, 2021). The GLIMS database at the National Snow and Ice Data Center can store outlines for both proglacial and supraglacial lakes; however, the lakes must be associated with glacier IDs and submissions are still scarce (Bruce Raup, personal communication 24 September 2021).

Glaciers in mainland Norway, hereafter referred to as Norway, have changed markedly since 2000 with pronounced retreat of glacier termini (Andreassen and others, 2020b). New satellite sensors such as Sentinel-2 (10–20 m) provide a higher spatial and temporal resolution than Landsat (15–30 m) (Kääb and others, 2016). This enables more detailed mapping and increases the chances of covering all glaciers over a shorter time span in an inventory (Paul and others, 2016). Sentinel-2 data have already been used to create a new inventory of the European Alps (Paul and others, 2020) and Iceland (Hannesdóttir and others, 2021) and to check inventory data derived with Landsat OLI data for New Zealand (Baumann and others,

2021). Although semi-automated methods using satellite imagery are now the most common, manual digitization of georeferenced high-resolution (0.25 m) aerial photographs for detailed glacier inventories are also used, such as for the entire Swiss Alps, and give the opportunity for mapping supraglacial debris cover (Fischer and others, 2014; Linsbauer and others, 2021).

In the past, glacier inventories have been compiled for glaciers in Norway. The first assessment was a detailed list of the numbers and areas of glaciers in Norway (Liestøl, 1962). This was followed by two detailed glacier inventories of southern Norway (Østrem and Ziegler, 1969; Østrem and others, 1988) and one of North Scandinavia (northern Norway and Sweden) (Østrem and others, 1973). These inventories were based on maps and aerial photographs, and consisted of tabular data and sketch maps displaying all identified glaciers. The first digital and satellite remote-sensing-based glacier inventory covering all of Norway was derived using Landsat TM/ETM+ scenes of 30 m resolution from the period 1999–2006 (Andreassen and others, 2012). Subsequently, two more digital inventories were constructed, one based on digitising 168 topographic map sheets based on aerial photographs from 1947 to 1985, and one based on nine Landsat TM4 and TM5 satellite scenes from 1988 to 1997 (Winsvold and others, 2014). However, the latter was not complete, e.g. not covering Jostedalbreen, due to severe snow and cloud conditions. Recent updates include glacier outlines from the 2010s using Landsat-8 OLI, but only for smaller glacier regions: Lyngen in 2014 (Stokes and others, 2018) and part of northern Troms and Finnmark in 2018 (Leigh and others, 2019, 2020). New outlines are also available from orthophotos and Pléiades imagery (0.25–2 m resolution) (Weber and others, 2019, 2020; Andreassen and others, 2020b). The inventory of southern Norway from 1973 and northern Scandinavia from 1988 (Østrem and others, 1973, 1988) contained information on glacier lakes as tabular entries, but the lakes themselves were not mapped.

The first digital glacier lake outline inventory of Norway was produced using Normalized Difference Water Index (NDWI) (Gao, 1996), topographic maps and manual edits using the Landsat images from the 1999–2006 glacier inventory (Andreassen and Winsvold, 2013). Additional lake inventories were constructed based on Landsat 1988–1997 and 2014 images using manual digitisation and the 1999–2006 lakes as a reference (Andreassen and Winsvold, 2013; Andreassen and others, 2021). An updated glacier lake inventory used NDWI and manual edits on Sentinel-2 images from 2018. This is the most recent and detailed lake inventory for Norway but does not include lakes located near glaciers smaller than 0.25 km² (Nagy and Andreassen, 2019).

Although many studies have published satellite-based inventories, validation methods for these inventories are not standardized. Methods such as the buffer method (e.g. Granshaw and Fountain, 2006; Paul and others, 2009; Meier and others, 2018) or the multiple manual digitisation of outlines by several qualified persons (Paul and others, 2013) are typically used to assess uncertainties, whereas high-resolution validation data to assess accuracy are more rare. Earlier comparisons of Landsat of 30 m resolution with orthophotos of 0.25 m resolution (Andreassen and others, 2008; Fischer and others, 2014) found relative area differences of 2–5% in mapped glacier area, however for smaller glaciers (<1 km²) relative differences were larger (Fischer and others, 2014). Paul and others (2020) used orthophotos to control Sentinel-2 outlines and to manually correct debris-covered glacier outlines in the Austrian part of their inventory.

The overarching aim of this study is to create new glacier outlines and ice-marginal lake outlines in Norway, which is underpinned by three research objectives: (1) to present appropriate methods for glacier delineation and classification, (2) to derive and validate the outlines, and (3) to test the sensitivity of the results. We use Sentinel-2 imagery to derive an updated dataset

of glacier outlines and ice-marginal lake outlines. To validate the outlines, we use very high-resolution aerial orthophotos (0.25 m) and Pléiades satellite data (0.5–2 m) for several test sites. We calculate the overall changes in glacier area since the previous 1999–2006 inventory. We assess the sensitivity of the results by applying the buffer method for all of Norway. We also compare our Sentinel-2 derived outlines of 10 m resolution with previously published outlines derived from a Landsat-8 pansharpened image of 15 m resolution for a subset of the glaciers.

2. Setting

Norway spans 13 degrees of latitude (from about 58 to 71°N, Fig. 1). In the previous inventory, 1999–2006, the total glacier area was 2692 ± 81 km² (using ±3% as uncertainty). The larger part, 1523 km² (57%), is in southern Norway, and 1169 km² (43%) in northern Norway (Andreassen and others, 2012). A total of 2534 glaciers (3143 glacier units when complexes are divided by ice divides) were defined in the inventory and categorized into 36 regions. In addition, ~400 polygons amounting to 24 km² were classified as ‘possible snowfield’ (PSF). Mass-balance measurements in Norway are currently conducted on a selection of ten glaciers and one ice patch, and length change measurements on 30–40 glaciers (Kjøllmoen and others, 2021). A recent review of glacier changes since the 1960s reveals an overall retreat of the glaciers, great inter-annual variability of mass balance and accelerated deficit and retreat since 2000 (Andreassen and others, 2020b). Some years with a positive (or less negative) mass balance after 2010 are attributed to variations in large-scale atmospheric circulation (Andreassen and others, 2020b). For a sample of 131 glaciers covering 817 km² in the ‘1960s’ and 734 km² in the ‘2010s’, the area reduction was 84 km², or 10% and the overall change in surface elevation was –15.5 m for the ~50-year period.

3. Data

3.1. Sentinel-2 scenes

The scenes used for glacier mapping are ideally acquired over a short time interval and have minimal seasonal snow and cloud cover (e.g. Raup and Khalsa, 2007; Racoviteanu and others, 2009). In the first years of the Sentinel era, 2015–2017, conditions were not optimal for glacier mapping in Norway due to too much snow. Scenes from August/September 2018 for northern Norway and August 2019 for southern Norway (Table S1) have less snow and cloud cover and were therefore used in this study. In total, 39 scenes were used: 34 of them were used for automatic mapping, and five were used for visual inspection (e.g. for small edits, but not used to automatically derive outlines). For some regions, multiple scenes had to be combined due to clouds obscuring the glaciers. For southern Norway, most of the scenes were taken from 27 August 2019, whereas scenes from 4 and 15 August 2019 were additionally used when glaciers were covered in clouds (Fig. 2). Earlier in the season, scenes had more seasonal snow, but had less terrain-induced shadowing due to the higher sun angle (e.g. Nagy and Andreassen, 2019). For northern Norway, most of the scenes were taken on 1 and 8 September 2018. Additional imagery from August 2019 and August/September 2018 was used when cloud coverage was unfavourable in the primary images. The glacier outline metadata describe data sources and dates used for the glaciers. In some cases, orthophotos were used due to clouds or severe terrain shadowing.

The Sentinel-2 scenes were downloaded as orthorectified scenes from the Norwegian National Ground Segment for Satellite Data (available at [satellittdata.no]). The orthorectified images are referred to as DTERRENG digital terrain model

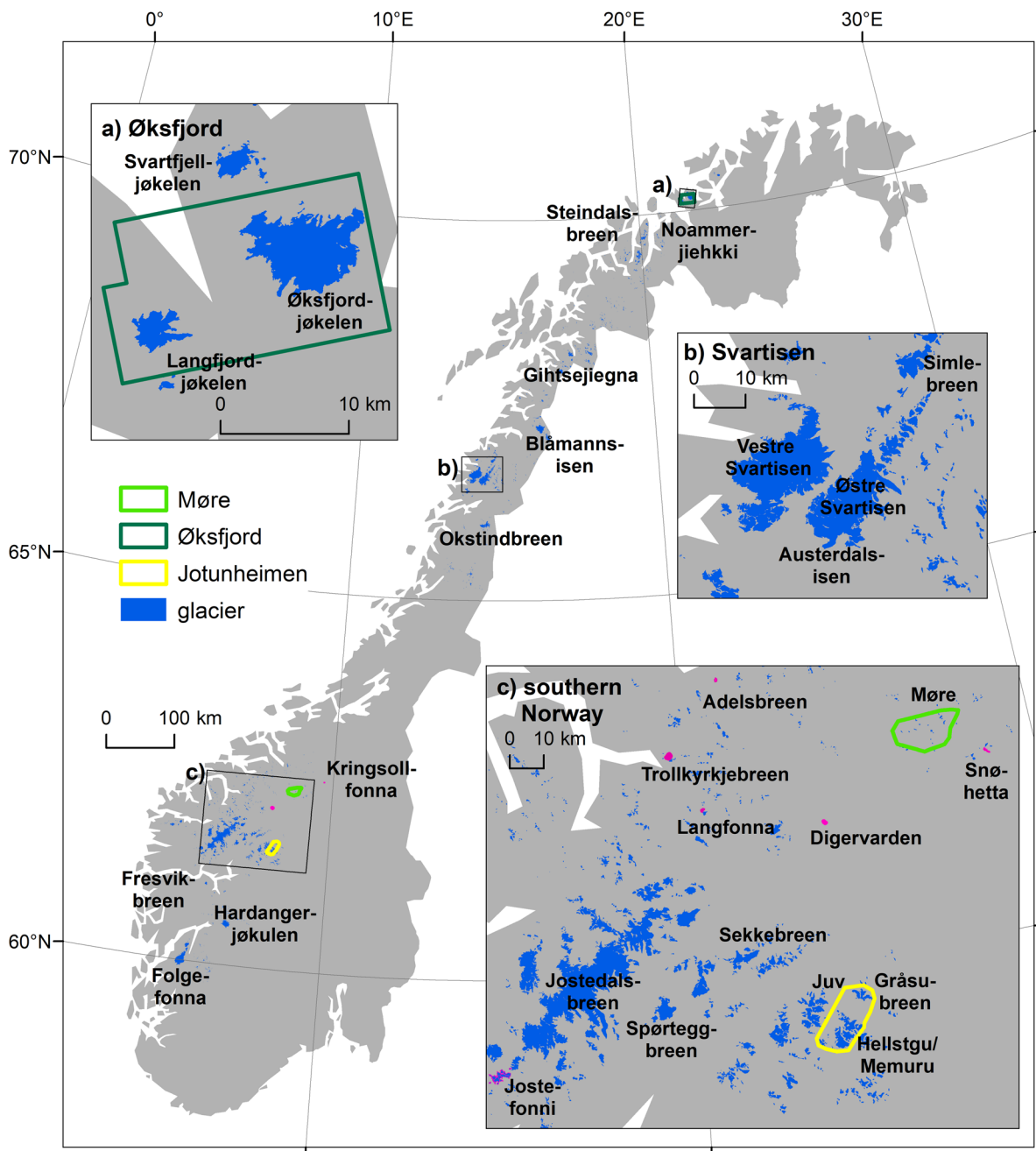


Fig. 1. Map of glaciers in Norway with names of many of the glaciers mentioned and extents of validation subsets referred to in this work. Pink colour shows the location of some of the smaller glaciers. Insets (a) Øksfjord, (b) Svartisen and (c) close up of some of the glaciers in southern Norway.

(DTM) data and are orthorectified using the national 10 m DTM of Norway. Geolocation errors are found in imagery orthorectified with the Planet DEM at the 90 m resolution for mainland Norway (e.g. Kääb and others, 2016; Andreassen and others, 2021). Images orthorectified with the 10 m DTERRENG DTM were therefore preferred. Sentinel images are typically displayed in red-green-blue (RGB) colour composites of three bands or as single bands. Composite images were created using five of the bands: blue (2), green (3), red (4), NIR (8) and SWIR (11). All the five composite bands are available at a 10 m resolution, except for band 11 that is originally available at a 20 m resolution but was resampled to 10 m resolution.

3.2. Orthophotos

Orthophotos (the most recent at the time of viewing) from the Norwegian mapping authorities were used directly as web map

service (wms) within the GIS and additional orthophotos were viewed in www.norgebilder.no. The photographs were used to control the result, and to check for ice content and the extent of smaller objects that were automatically mapped from the Sentinel-2 imagery. Orthophotos originated from many different dates. Photographs taken several years prior to the Sentinel-2 scene used could not be used to directly control for glacier extent in 2018–19, as many glaciers have retreated in recent years (Andreassen and others, 2020b; Kjølmoen and others, 2021).

For some regions (Folgefonna, Hardangerjøkulen, Hardangervidda and Møre), new orthophotos from 2019 were available, the same year as the Sentinel-2 scenes used for the glacier mapping. Selected photos were downloaded and used for direct validation (Section 4.5). Snow conditions around the glaciers and the glacier extents vary during the summer as melting progresses or snowfall occurs. Whereas the 2019 Møre orthophotos were taken on the same day as the Sentinel-2 image and could

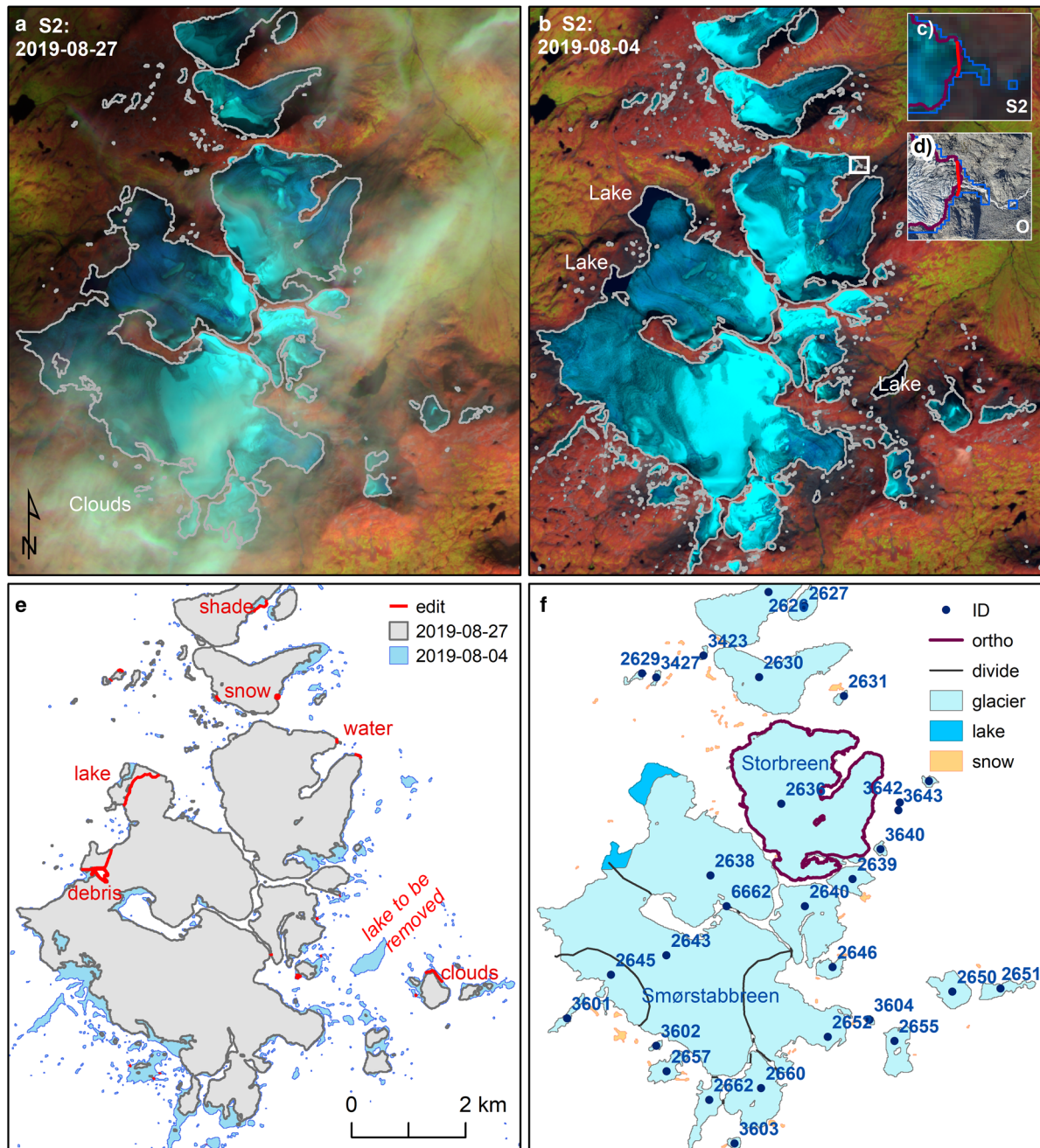


Fig. 2. Sentinel-2 images (false 11-8-4) of (a) 27 August and (b) 4 August 2019 and automatically derived outlines (grey and blue respectively). Due to cloud cover both scenes were used to derive glacier and glacier lake outlines. (c) Part of the Storbreen tongue where both a river and ice blocks had to be removed using manual line edits. (d) Orthophoto of 26 August 2019 used to manually digitise the glacier polygon (ortho). (e) Automatic mapping result shown with line edits. (f) Final results of classified glaciers and snow, ID points and ice divides. /Copernicus Sentinel data 2019/.

be used for direct validation, most of the other 2019 photos were taken in late September after snow falls covered much of the glacier surfaces and perimeters making the orthophotos less informative (Fig. 3). For other regions, such as Jostedalbreen, Breheimen and Jotunheimen, the most recent images were from 2015 or 2017 where snow conditions were often adverse with much seasonal snow (Fig. 3). For Fresvikbreen, the most recent images were from 19 July 2017 and had poor contrast and considerable seasonal snow cover (Fig. S1). Earlier images from 27 September 2010 were taken in a year with high melting and little seasonal snow remaining, but unfortunately a snowfall covered the surface prior to the time of the photograph being taken. For this glacier, the 19 September 2006 orthophoto provided the most information to assess ice content and glacier features. Such out-of-date images with good mapping conditions could still be useful to

check the Sentinel-2 outlines in the accumulation regions with shadow, bergschrund and for the overall topography.

We also had orthophotos with a 0.25 m resolution from targeted glacier surveys of Jotunheimen taken on 26 August 2019 for the Norwegian Water Resources and Energy Directorate (NVE). This survey was conducted one day before the Sentinel-2 scene of 27 August 2019 that was used to map most of the glaciers in this region.

3.3. Other datasets

Other datasets we used were:

- Satellite orthoimages derived from Pléiades scenes (© CNES 2019, Distribution Airbus DS). The two scenes we used were acquired

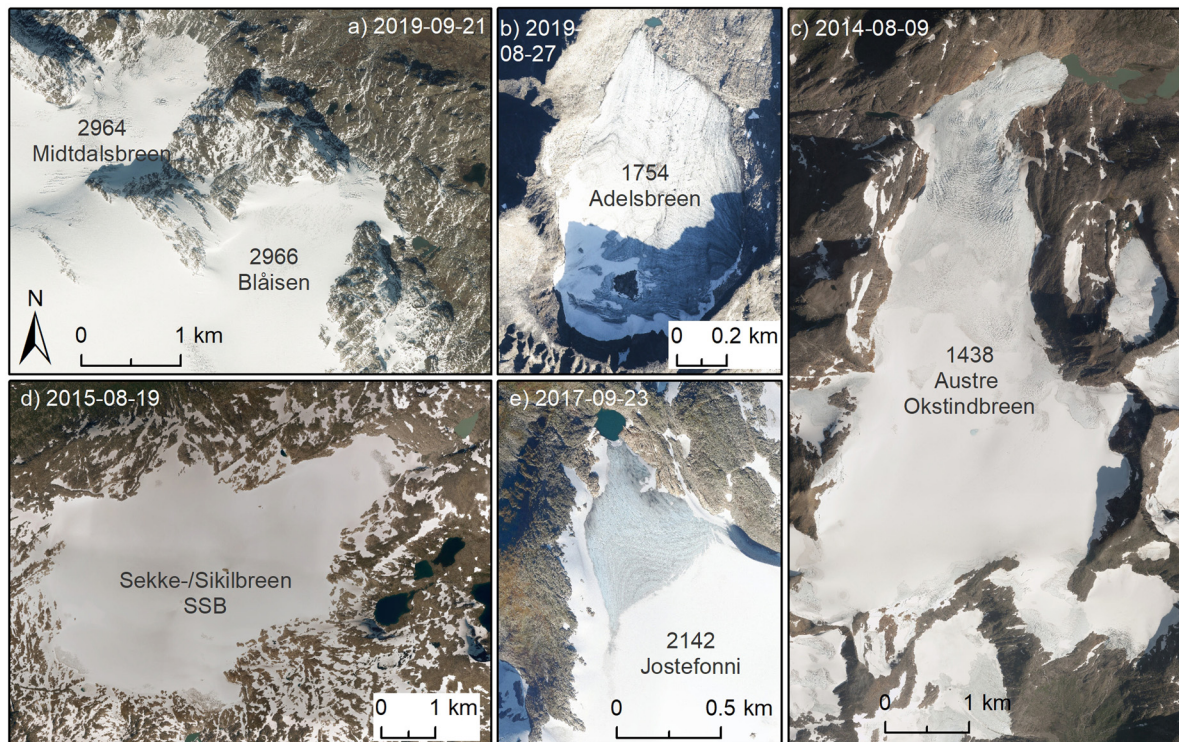


Fig. 3. Snow conditions and time of mapping varied greatly in the recent orthophotos from www.norgebilder.no that were used to check the results from the Sentinel-2 mapping. (a) Part of the Hardangerjøkulen photo taken 25 days after the Sentinel-2 scene, glaciers are covered by fresh snow. (b) Adelsbreen, Møre, photo taken on the same day as the Sentinel-2 scene. (c) Part of Okstindbreen, photo taken 4 years earlier than the Sentinel-2 scene, (d) Sekkebreen, photo taken in 2015, a year with much seasonal snow remaining in southern Norway. (e) Part of Jostefonni, 2 years prior to the Sentinel-2 scene, seasonal snow still covered the glacier perimeter. All images © Norgebilder.no. See Table S2.

near the time of the Sentinel-2 scenes used for the glacier mapping and were therefore optimal for validation of the outlines. One scene covered Øksfjordjøkelen and Langfjordjøkelen and was acquired 1 September 2018. The other scene covered parts of Jotunheimen and was acquired 27 August 2019. The scenes were available in 0.5 m (panchromatic) and 2 m (multispectral) resolution.

- The 10 m national DTM from the Norwegian mapping authorities.
- Standard topographical data of Norway (administrative borders, lake, land cover, elevation contours, etc.) as vector layers and as wms from the Norwegian mapping authorities.
- NVE's glacier inventory from 1999 to 2006 including over 400 PSF polygons without glacier ID (Andreassen and others, 2012).
- NVE's glacier lake inventories from 1999 to 2006, 2014 and 2018 (described in Andreassen and others, 2021 and references therein).

4. Methods

4.1. Glacier delineation

To map the ice bodies, we applied a standard band ratio method with a threshold on the selected Sentinel-2 scenes. This method uses threshold values and should be optimized for each satellite scene; however, the optimum threshold can be difficult to find and can vary also within a scene (Paul and others, 2016). Two thresholds were used. A band ratio threshold (T1) was calculated as the red band 4 divided by the shortwave infrared band 11 (SWIR). A threshold in the blue band 2 (T2) was used to improve classification in shadow (Paul and Käab, 2005; Paul and Andreassen, 2009; Winsvold and others, 2014; Paul and others, 2020). A median filter of 3×3 pixels kernel (30×30 m) was thereafter applied to reduce noise in shadow and remove isolated

pixels. Then the selected thresholded result was converted to polygons. We incremented the band ratio and band thresholds with steps of 0.2 and 50, respectively, to find an optimal combination (Fig. 4). To include the dirty ice around glacier perimeters, T1 should be kept as low as possible (Paul and others, 2013). Some of the smallest glaciers or possible snow fields may not be mapped for large values of T1 and T2 (Winsvold and others, 2014). In our study, selected values of T1 varied between 2.0 and 3.0 and selected values of T2 varied between 1000 and 1200 (Table S1). In Jotunheimen, we chose a low value of T2 (1000) so as to not underestimate the shadowed parts (Fig. 4). For debris-free ice, the result was not very sensitive to the thresholds chosen (Fig. 4). Generally, less ice is mapped with a large band ratio threshold. The results were checked glacier-by-glacier using the orthophotos and Sentinel composites of natural colour (4-3-2), false colour composites (8-4-3 and 11-8-4) and single bands. Band 2 was useful for parts in shadow. Geolocation errors were found in some of the orthophotos. The Sentinel-2 scenes were in any case the primary source for the glacier and glacier lake outlines. Therefore, when editing and checking the datasets, the Sentinel-2 images were preferred as a background for consistency, whereas the orthophotos were used for familiarising oneself with the region and cross-checking (potential) ice content. Topographic maps were used as both wms and vector layers for identifying new glacier names and general topography (Fig. 5). The lake and land vector data of Norway were used to remove water bodies that were included in the automated mapping.

Where edits were needed, these were digitised as line segments and an edit code was associated with the line segment. The line segment was used to modify or cut the polygon. In this way, it was possible to track the edits that were made (Fig. 2).

Manual corrections are typically needed for water bodies, debris cover, shadow, snowfields and ice on water (e.g. Paul and

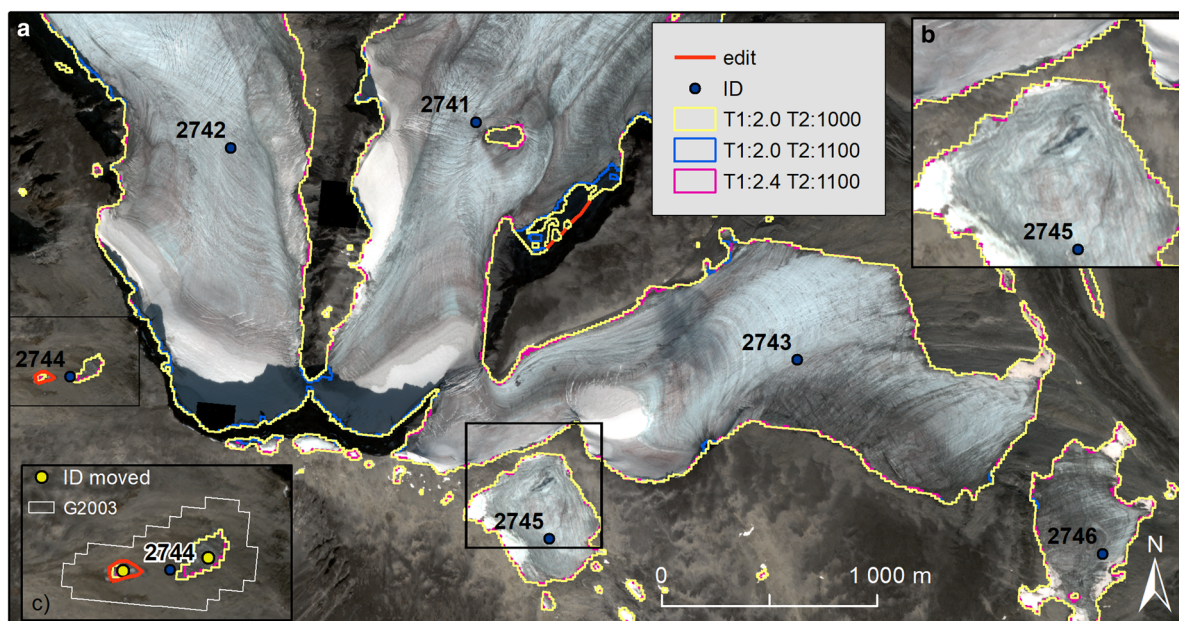


Fig. 4. (a) Three automatically derived outlines with values of T1 and T2 for a subset of Grjøtbreen (2742 + 2741) and Gråsubreen (2743) in Jotunheimen from a Sentinel-2 scene from 27 August 2019 compared with a Pléiades image of the same date. (b) Detailed part of Glitterbreen and Gråsubreen. There is no difference between T2 1100 and 1000 in this part. (c) A small ice patch (ID 2744) that disintegrated since 2003 and where the ID was moved. The smallest part was manually edited in this case. The T1: 2.0 and T2:1000 were used as the final outline with edits. Many of the smaller polygons were not included in the final inventory. /Pléiades © CNES 2019, Distribution Airbus DS.2019/.

others, 2009). As in the previous 1999–2006 inventory, the main corrections were inclusion of shaded areas and editing at the glacier-lake interface (Andreassen and others, 2012). Most glacier regions across Norway have little supraglacial debris. However, in areas of steep terrain (e.g. Lyngen, Jotunheimen, Møre and Sunndal which are dominated by small cirque and valley glaciers), supraglacial debris is more prominent and some debris-covered parts were corrected using manual digitisation. Moreover, automatically mapped holes (nunataks) were closed when they were likely to be debris. This was difficult to judge from the Sentinel-2 images alone, so uncertainties remain for smaller nunataks. It was also difficult to control parts in heavy terrain shadow, which also may include debris cover. Images captured earlier in the year (e.g. early summer) proved useful in determining areas prone to heavy shading, but determining glacier extent remained challenging where debris cover was present. Such debris-covered extents will have larger uncertainties. Seasonal snow was, as in previous inventories of Norway, a challenge especially along the margins of a glacier where it can persist late into, and sometimes throughout, the melt season (Fig. 3). In some cases, this was cut out and marked as snow (Fig. 2) but it can be difficult to separate snow from disintegrating ice. To keep such edits to a minimum, continuous polygons were mostly kept as is.

4.2. Glacier classification

A glacier can be defined as ‘a perennial mass of ice, and possibly firn and snow, originating on the land surface by the recrystallization of snow or other forms of solid precipitation and showing evidence of past or present flow’ (Cogley and others, 2011). We followed the same overall structure as in the previous inventory and divided the bodies into glaciers, ice patches or snow (Andreassen and others, 2012). Snow was excluded but kept in a separate layer so it could be used in other applications or reselected if needed. Thanks to the higher resolution of Sentinel-2 (10 m) over Landsat (30 m) used in the 1999–2006 inventory, smaller

items could be mapped. In the 1999–2006 mapping, the lower threshold was nine pixels, equivalent to 8100 m² (0.0081 km²). With Sentinel-2, we selected nine pixels as the initial threshold, thus only 900 m². As glaciers are shrinking and disintegrating even such small polygons can contain ice. All bodies larger than nine pixels were inspected by at least checking the Sentinel images. Many of the smaller polygons (<4000 m²) were quickly classified as snow based on topography and elevation in the region. As smaller ice bodies are also of interest in Norway, e.g. due to archeological finds that have been numerous on many small bodies since 2006 (e.g. Nesje and others, 2012; Pilø and others, 2021), we decided not to have a higher threshold. A test of ten archeological sites of interest showed that small ice bodies can be mapped with reasonable accuracy using Sentinel-2 images (Andreassen and others, 2020a). Furthermore, small polygons were often indicators of glaciers or ice patches in shadow (e.g. in cirques) that were not fully detected by the algorithm. Thus, by keeping this low size threshold, we detected several smaller glaciers in shadow and manually edited them. When recent orthophotos were not available or the mapped body was totally snow covered, the classification was based on previous classification, and appearance of ice in the Sentinel-2 image. Size is often used as a criterion for defining an ice body as a glacier, but some very small bodies in steep terrain can have ice content and crevasses. On the other hand, snow bodies can be large and have no ice content, but snow patches in steep terrain may have snow crevasses due to gravity.

Leigh and others (2019) used Landsat imagery and orthophotos from norgebilder.no to map glaciers in glacier regions 2 (Øksfjord) and 3 (Troms – North) (Andreassen and others, 2012). They proposed a scoring system that can be used to classify glaciers in categories as certain, probable, possible and perennial snow. Scores of 1–5 points (maximum 20 in total) are given based on the appearance of crevasses, flow features, ice, etc. (Table S3). For example, a body with crevasses, deformation features and visible areas of ice will score >10 points and be classified as ‘certain’. A body that has ice and features indicating past flow

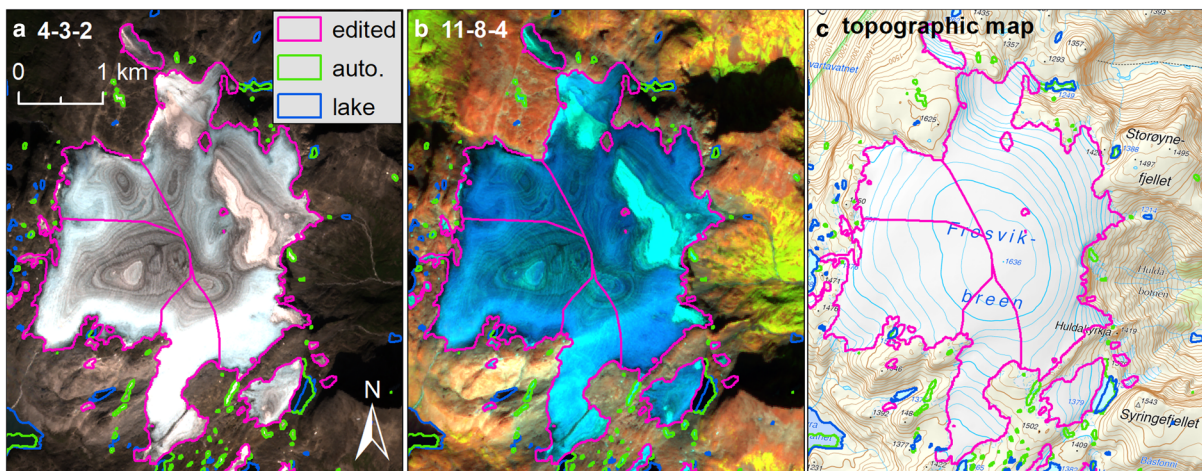


Fig. 5. (a) Sentinel-2 scene from 27 August 2019 for Fresvikbreen displayed in natural colours (band 4-3-2) and (b) false colours (band 11-8-4), with automatically (auto.) derived outlines and edited outlines (removal of lakes and snow and other edits). Lake: lake layer from the topographical main map series of Norway (N50). (c) The topographic map as wms from the Norwegian mapping authorities was used to check glacier names and topography. For Fresvikbreen orthophotos from 2017 (extensive snow cover), 2010 (fresh snow) and 2006 (minimal snow) from © Norgebilder.no were also checked (Fig. S1). /Copernicus Sentinel data 2019/.

will score as a 'probable' glacier and be classified as an ice patch or ice remnant. A body of ice with no presence of flow features or deformation will be categorized as 'possible'. The advantage of this method is that it can be used objectively to categorize mapped bodies. The disadvantages are that it requires recent orthophotos and is a manual and time-consuming method. It is also difficult to differ between perennial and seasonal snow, as few of the orthophotos are taken at the end of the season (Fig. 3). In our study, we tested the scoring principles by Leigh and others (2019) in a subregion (see Section 6.1). We also leaned on the classification criteria to aid the assignment, without assigning individual scoring points to each body.

4.3. Glacier attributes

For comparison purposes, we decided to use the ice divides from 1999 to 2006 as far as possible. Glacier divides were updated for some glaciers to fit with divides used in NVE's mass-balance calculations (Fig. S2). Some other minor edits were carried out, mainly to separate units more naturally. On many of the smaller glaciers, the 1999–2006 ice divides were not needed for the 2018–19 dataset due to glacier shrinkage or the fact that the Sentinel-2 resolution of 10 m was much better at separating neighbouring glaciers compared to the 30 m Landsat resolution. Glacier ID points were kept as is but moved if they were no longer within the glacier polygon or close to the polygon border due to glacier shrinkage. In cases where the glacier had disintegrated to several parts, the point was moved to the largest remnant or most 'glacier-like' remnant (Fig. 4c). This was done using topology editing and manual inspection in the GIS (©ArcMap 6.1). Each polygon was assigned a unique ID for 2018–19 that was either new or inherited from 1999 to 2006. All polygons within the 1999–2006 glacier extent inherited the 1999–2006 glacier ID as a secondary ID. In this way, one can calculate observed changes and have a unique identifier.

4.4. Glacier lakes

The semi-automated method used for glacier outline mapping in our study often requires manual edits to detach glacier lakes connected to the glacier outlines (Fig. 2). Thus, we produced an updated glacier lake outline dataset for 2018–19 to match the new 2018–19 glacier outlines. We included additional lakes for

glaciers smaller than the 0.25 km² threshold for glacier size that was set for the 2018 product (Nagy and Andreassen, 2019). For northern Norway, the glacier lakes were used as in the 2018 product, with some corrections and additions of lakes at glaciers below the 0.25 km² glacier size threshold. The Sentinel-2 scenes used for the 2018 mapping were taken earlier in the season than the glacier outline mapping. This had the advantage of less terrain shadows but the disadvantage of more snow and ice remnants at the glacier perimeter and lake surface.

For southern Norway, we updated and mapped the lakes using the 2019 imagery. The glacier outline-lake interface was manually digitized as a line based on the Sentinel-2 imagery used for the glacier outline mapping. Each digitized lake interface line was given an edit code for 'glacier lake', and the glacier lake was detached from the glacier by splitting the mapped polygon with the digitized line. This often resulted in a polygon partly covering the glacier lake. To map the full glacier lake extent, the automatically mapped glacier lakes were either modified, extended with manual edits or merged with the 2018 outlines or lakes from the topographic map series 1:50 000 of Norway. Orthophotos from norgebilder.no or other Sentinel-2 imagery were used to verify glacier lakes where newer photos were available, however not all lakes could be verified due to snow conditions, lake ice, or lack of recent orthophotos. For some of the smaller glacier lakes, the outline was automatically mapped and used 'as is' after splitting, while other parts of the lakes were manually digitized. Supraglacial lakes were also manually digitized. Large lakes were often easy to detect, while small and newly formed lakes were more difficult to identify and thus more uncertain. The lakes appeared dark in false colour composites compared to snow and ice, but very small glacier lakes were difficult to differentiate from debris, shadow or braided rivers. Lake colour also varied due to sediment content and lake size and shape (e.g. Matta and others, 2017; Nagy and Andreassen, 2019). For this lake inventory, we included lakes that were likely to be in contact with the glaciers at the time of satellite image acquisition.

4.5. Validation

To validate our Sentinel-2 semi-automated mapping, we compared our data with manual digitisation from aerial orthophotos of selected glaciers in Jotunheimen, Møre, Dovre and Hardangerjøkulen (0.25 m resolution) and Pléiades orthoimages

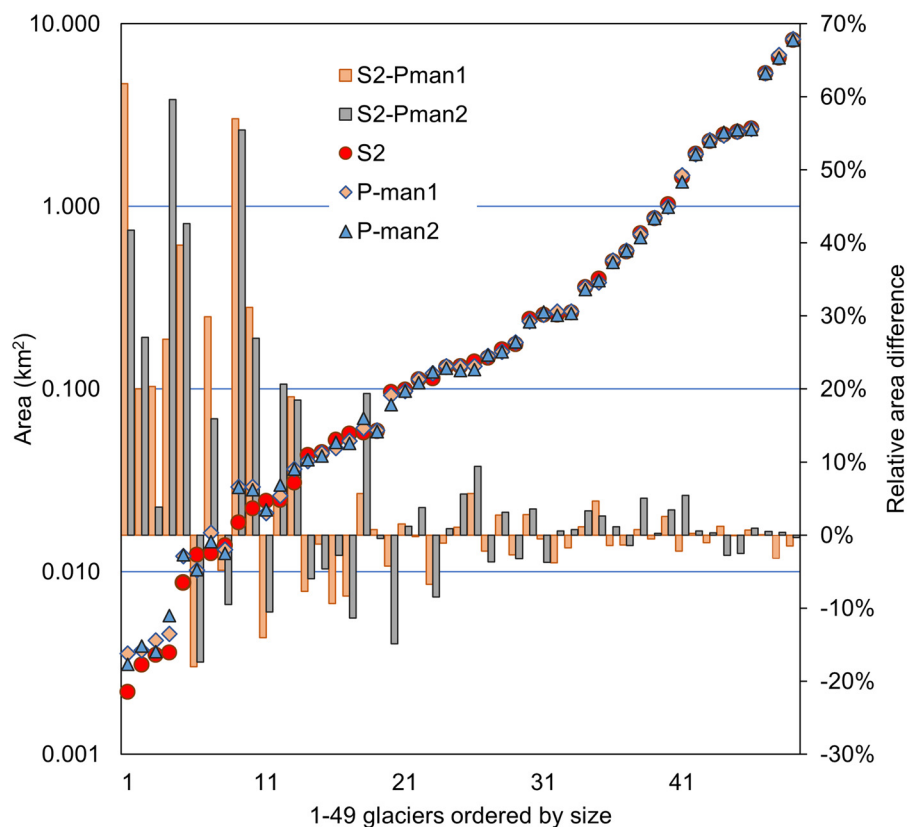


Fig. 6. Area derived from Sentinel-2 (S2) vs two independent manual digitisations from Pléiades imagery (P-man1 and P-man2) for a subset of 49 glaciers in Jotunheimen. Relative area differences are also shown. See Figures 4, 7 and 8 displaying some of the glaciers. Note that the scale is logarithmic on absolute left y-axis.

(0.5–2 m resolution) available for a subset in Jotunheimen and Finnmark. Below, we describe five validation cases. The manual digitisation described here was done independently of the Sentinel-2 mapping. An orthophoto or orthoimage was the only product available for the digitiser except for Langfjordjøkelen (case 4.5.1). Results from the validation and other sensitivity tests are summarized in Table 7 in Section 6.3.

4.5.1. Pléiades orthoimage and aerial orthophotos for a subset of Jotunheimen

In the first evaluation, a subset of the Pléiades scene of 27 August 2019 (0.5 and 2 m orthoimage) was used. The scene was acquired the same day as a Sentinel-2 scene used for the glacier mapping. Two of the authors independently digitised the glaciers manually. These were then compared with the final Sentinel-2 outlines for a total of 49 glaciers or ice bodies ranging from 0.002 to 8.1 km² in area (Figs 4, 6–8). Some of the glaciers were mapped as two bodies in the Pléiades digitising, and one body by the Sentinel-2 algorithm (Fig. 7b). We compared the area sum of the bodies, and results revealed that the mapped glaciers differed between the two authors. Some smaller bodies were mapped by one author only. Some of the bodies were not included in the Sentinel mapping. The total area of the mapped ice bodies by the two authors using Pléiades was 40.95 and 40.52 km², respectively, while the results from using Sentinel-2 was 40.63 km². Thus, the Sentinel-2 area was 0.28% smaller or 0.78% larger compared to Pléiades reference. It is noteworthy that the Sentinel-2 estimate lies between those from Pléiades and that the Pléiades estimates for individual glaciers have larger variations (Fig. 6).

For a selection of glaciers in the Pléiades subset we had orthophotos taken on 26 August 2019 (0.25 m resolution), the day before the Sentinel-2 and Pléiades imagery. These glaciers were digitised by two of the authors (one digitisation per glacier). In total, 15 smaller and larger ice bodies were mapped, ranging in size from 0.01 to 8.16 km². The total glacier area derived from

the orthophotos was 19.59 km², whereas the total glacial area derived from the Sentinel-2 was 19.53 km², which represents a 0.3% difference. Of the ten glaciers in the sample larger than 0.1 (0.3) km², amounting to 99 (96) % of the area, the relative differences were within ±4%. The glaciers smaller than 0.1 km² had relative differences ranging between –66% (for the smallest glacier) and 9%. The three datasets (Pléiades, Sentinel-2 and aerial orthophotos) were taken with a 1-day time difference and melting along the perimeter is considered negligible. Results for Gråsusnippen (ID 2746), a 0.4 km² ice patch, revealed that manual digitization attempts between the two authors differed by 2–5%. Differences were mainly due to decisions by the observer on what to include in the perimeter (Fig. 8). Using 2.4 as threshold T1 instead of 2.0 would reduce the area by 0.016 km², or 4%. The area of Gråsusnippen ranges between 0.401 and 0.382 km² for the various methods and rounds to 0.4 when using one decimal.

4.5.2. Glaciers around Snøhetta, Dovre

Three glaciers around the Snøhetta peak (Dovre, Innlandet county) were digitised by one author using orthophotos from 27 August 2019 from norgebilder.no, the same day as the Sentinel-2 scene. The Sentinel-2 outlines were edited in areas of terrain shadow and at the terminus of one glacier (Fig. 9). The terrain shadowing and supraglacial debris made mapping in this region challenging. Some parts were corrected when cross-checking with the orthoimage and Sentinel-2 image. The total area of the three glaciers was 1.53 km² for the orthophoto, 1.50 km² for the Sentinel-2-edited and 1.40 km² for the automatically derived product (Table 1). In the Snøhetta case, the automatic mapping resulted in the smallest areas, as parts in shadow were not mapped. The manually digitised outline from the orthophotos gave a 2.0% larger area than the corrected Sentinel-2, and a 9.5% larger area than the automatically derived outline. This illustrates

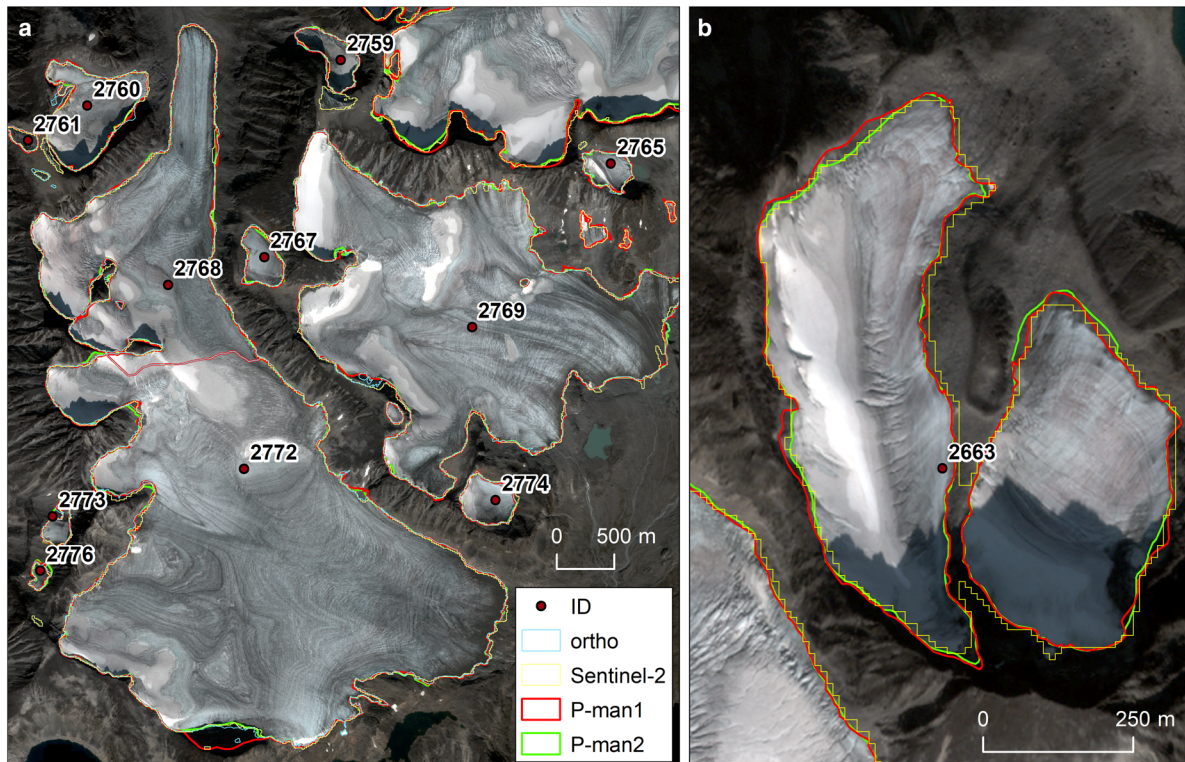


Fig. 7. Subset of the Pléiades scene of 27 August 2019 showing (a) Hellstugubreen (2768) and surrounding glaciers, and (b) glacier ID 2663. Figure 7a has one more outline (ortho), derived from orthophotos from 26 August 2019. /Pléiades © CNES 2019, Distribution Airbus DS/.

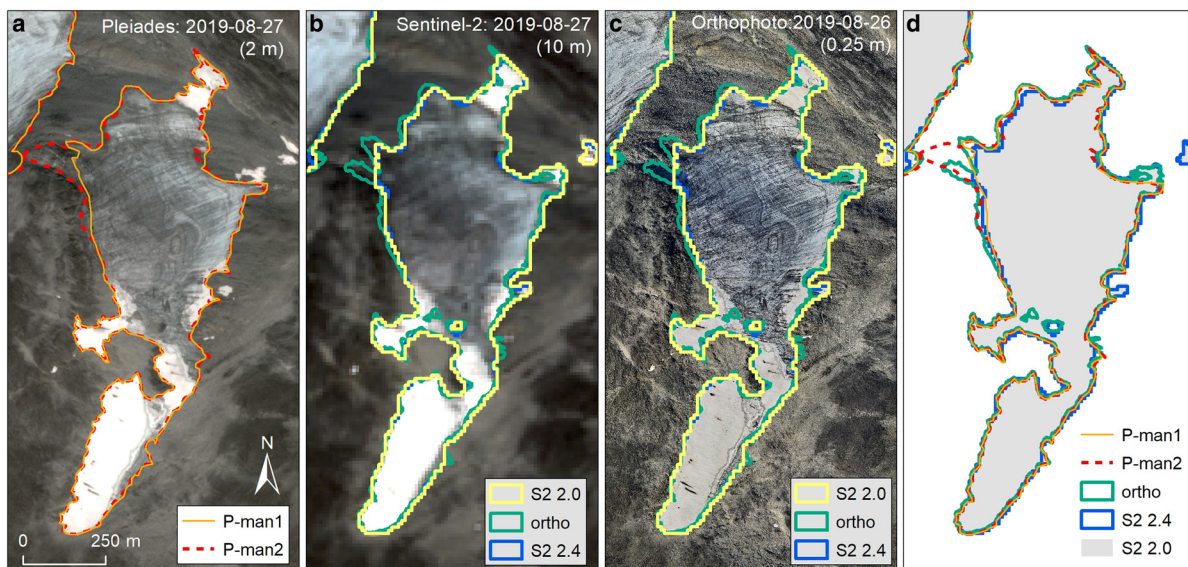


Fig. 8. Gråsusnippen (ID 2746) as mapped by manual digitisation of Pléiades image (P-man1 and P-man2), semiautomatic from Sentinel-2 (S2 2.0 and 2.4) and manual from orthophoto (ortho) together with resulting outlines. Here the largest difference is in the interpretation of dark ice in the north-western part. (a) Pléiades image, (b) Sentinel-2 (natural 4-3-2), (c) Orthophoto and (d) resulting outlines. /Pléiades © CNES 2019, Distribution Airbus DS. /Copernicus Sentinel data 2019/.

how glacier areas can be underestimated in shaded or debris-covered parts.

4.5.3. Ice patch at Digervarden

The Digervarden ice patch is of interest due to an archaeological ski find in 2014 (Finstad and others, 2018). The ice patch was mapped with Landsat for the 1999–2006 inventory but was only included in the PSF layer stored in the NVE database (Fig. 10). The area mapped from the Landsat image taken on 9 August

2003 was 0.173 km², whereas the area of the five ice bodies automatically mapped using Sentinel-2 from 27 August 2019 was 0.055 km². A comparison of Sentinel-2 derived outlines with orthophotos from the same date revealed that the automatic mapping algorithm did not always capture the full perimeter along very thin and dark ice (typically remnants of ice and disintegrating parts) (Fig. 10). The manually digitized outlines from orthophotos (Fig. 10) resulted in a larger total area of 0.076 km². The area of the two smaller items not included in Sentinel-2 mapping

Table 1. Resulting areas (A) of automatic mapping of Sentinel-2 (S2or), edited mapping (S2ed) and manually digitised from orthophoto (Ortho) and relative area differences ΔA between S2ed or S2or and Ortho (O), for the Snøhetta glaciers

ID	S2or A (km ²)	S2ed A (km ²)	Ortho A (km ²)	S2or – O ΔA (%)	S2ed – O ΔA (%)
1734	0.388	0.463	0.436	–12.3	5.8
1736	0.156	0.163	0.184	–18.4	–12.9
1738	0.856	0.877	0.912	–6.6	–4.1
Total	1.400	1.503	1.533	–9.5	–2.0

was 0.006 km². They were also detected by the automatic mapping but were not included due to their insufficient size of four pixels. The total area of the present ice patch parts was 0.021 km², 38%, larger than as mapped with Sentinel-2. Our Sentinel-2 mapping did not capture all parts of small bodies with dark surfaces. In detailed studies of such bodies, it is possible to manually digitize more ice from the Sentinel-2 images or fine-tune the thresholds.

For 2018–19, we selected one T1 and T2 threshold per scene ranging from 2.0 to 3.4 for T1 and 1000 to 1200 for T2 (Table S1), whereas the optimal threshold will vary through the scene (Paul and others, 2016). In this case, the orthophoto was the best source for a detailed outline, but Sentinel-2 has the advantage of a much higher temporal coverage, allowing us to follow the seasonal and annual changes (Andreassen and others, 2020a). In our overall manual edits, we added more ice in some cases (Fig. 4; inset 2744). However, in many cases, we did not have such validation data, and to obtain a consistent dataset and reduce the manual edits, we did not overedit such parts. Although the percentage differences may have been large, the excluded parts only contributed to a small area and ice volume.

4.5.4. Glacier and glacier lake Langfonna and Hardangerjøkulen

We also tested our semi-automated lake mapping with manual digitisation by two of the authors for two sites (Fig. 11). At Langfonna glacier (ID1864) in Møre og Romsdal, the lake area of the Sentinel-2 scene from 15 August (0.235 km²) coincided within $\pm 1\%$ of the digitisation from orthophotos (0.232 and 0.234 km²) from 27 August 2019 (Table 2). For the glacier area, the difference was larger. The Sentinel-2 area was 0.374 km² and the manual digitisation was 0.348–0.360 km². This corresponds to a 4–7% smaller area, which was mainly due to less snow being included and less glacier area mapped in the steep part on the eastern rim. Some of the difference may also have been due to snow melting between 15 and 27 August 2019 (the image of 27 August 2019 had clouds and was not used).

An additional test was carried out by digitising the glacier-dammed lake Demmevatnet at the outlet glacier Rembesdalskåka and three other ice-marginal lakes in the western part of Hardangerjøkulen (Fig. 11b). Here, the area of lake Demmevatnet was within 1% of the Sentinel-2 derived lake areas, whereas the three other lakes varied between 3 and 16%. Demmevatnet was drained in a GLOF event on 24 August 2019 and was thus empty at the time of mapping the glacier outline and lakes 2–4 (Fig. S3). Therefore, the earlier image from 4 August was used for Demmevatnet (Fig. S3). The largest relative area difference was for the smallest lake in the sample (lake 2). The largest difference in absolute area was for lake 4, with differences of –0.007 and 0.008 km². Floating ice was included in one of the manual digitisations from orthophoto but excluded in the other manual and in the Sentinel-2 manual correction. In cases with floating ice or ice bergs close to the ice-lake interface, the lake outline was more uncertain.

Our testing revealed that glacier lakes can be mapped accurately from Sentinel-2 using our semi-automated approach. The

lakes are clearly visible and easy to detect once they reach a size of ~ 0.1 km², but smaller lakes are more uncertain. Based on our experience using NDVI and manual digitization on the Sentinel-2 image, the accuracy in manual mapping or semi-automated mapping as used here is as good as or better than the automatic approaches and can be faster, at least for a region such as mainland Norway.

4.5.5. Glacier extents of Øksfjordjøkelen and Langfjordjøkelen

Pléiades images available for two ice caps in Finnmark, Øksfjordjøkelen and Langfjordjøkelen were used to digitise the glacier outlines (one outline per glacier). The resulting area derived from manually digitised outlines was 35.9 km² for Øksfjordjøkelen and 6.2 km² for Langfjordjøkelen, while the results from the semi-automated mapping were 36.3 and 6.4 km², respectively (Fig. 12, Fig. S4). It should be noted that for the Sentinel-2 imagery-based outlines for Landfjordjøkelen, the Pléiades images and outlines were compared when deciding the T1 and T2-values and as such, these outlines are not independent. The area difference between Pléiades and Sentinel-2 for Øksfjordjøkelen and Langfjordjøkelen of 1.2% (0.44 km²) and 3.1% (0.20 km²), respectively, point to what can be expected when mapping Norwegian ice caps with relatively clean ice but with some shadow issues.

5. Results

5.1. Total area and number of glaciers

The total area of glaciers mapped in the new 2018–19 inventory of Norway is 2328.4 km². This includes 2375 ‘newly’ mapped ice bodies totalling 48 km². The ‘new’ bodies range in size from <0.001 to 0.205 km² and 23 of them are larger than 0.1 km². When excluding those mapped as PSF in 1999–2006 (e.g. Digervarden, Fig. 10), there are still over 2000 ‘new’ bodies totalling 37 km² with nine larger than 0.01 km². Mapped snow polygons not included in the 2018–19 inventory represented an area of 98 km² in total. Glaciers with a size of >5 km² (>1 km²) >0.5 km² amount to 46% (78%) 85% of the total area. Glaciers and ice bodies smaller than 0.1 km² amount to 5.6% of total area and 75% of the total number. A total of 60% (1399.9 km²) of the glacier area is in southern Norway and 40% (928.5 km²) is in northern Norway (Table 3). For the ten largest glacier complexes (glaciers not divided into glacier units), the total area is 1214.2 km² in 2018–19 and they represent 52% of the total area. Glaciers in Norway are mainly found in the counties Vestland (1077 km², 46% of total glacier area), Nordland (722 km², 31% of total area), Innlandet (247 km², 11% of total area) and Troms and Finnmark (207 km², 9% of total area). These four counties contain 97% of the total area (Fig. S5). Norway and Sweden are divided into three GTN-G (RGI) subregions in glacier region 8 Scandinavia (GTN-G, 2017) (Fig. S5). The glacier region 08-01 (N Scandinavia) contains 928 km² (40% of total Norway), 08-02 (SW Scandinavia) contains 1137 km² (49% of total) and 08-03 (SE Scandinavia) contains 263 km² (11% of total). Whereas the two GTN-G subregions 08-02 and 08-03 are fully covered by our inventory, the 08-01 region lacks the Swedish glacier area.

5.2. Glacier area change from 1999–2006 to 2018–2019

The total glacier area of Norway declined from 2692 km² in 1999–2006 to 2328 km² in 2018–2019, which is a reduction of 364 km², or 13.5%. Including the PSF layer mapped for 1999–2006 gives a total area of 2716 km² and thus a reduction of 388 km² or 14.3%. The 3143 glaciers included in 1999–2006 had a total area of 2281

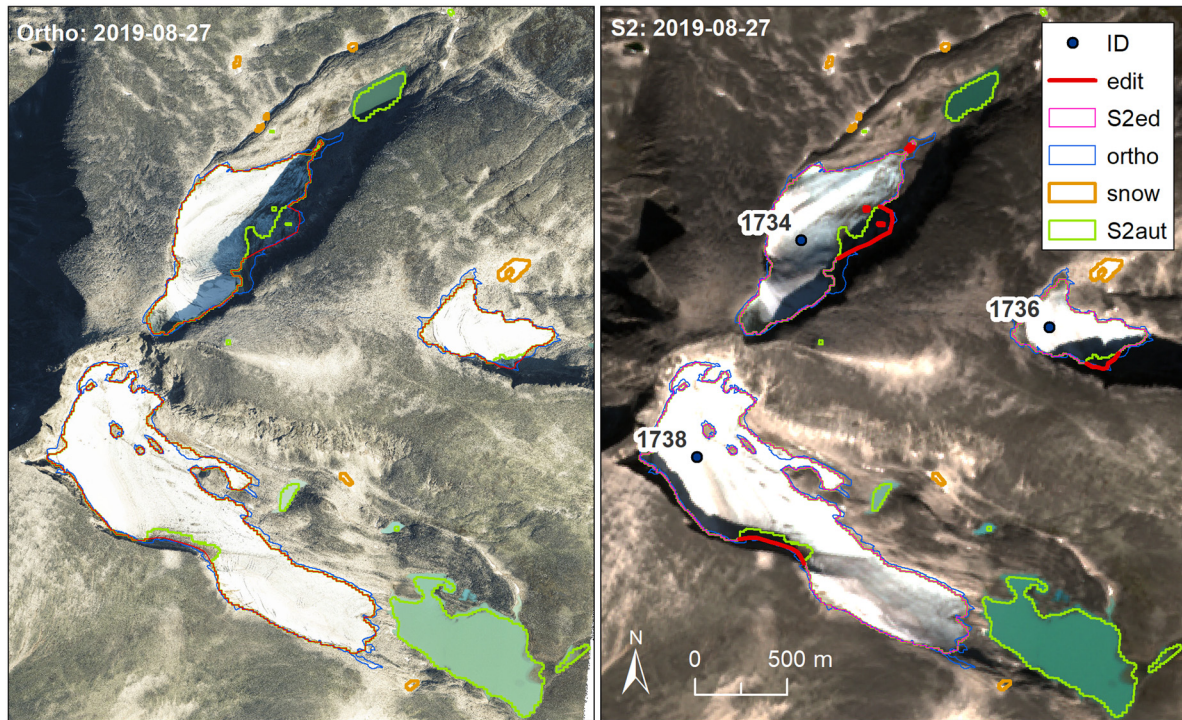


Fig. 9. Glaciers at Snøhetta as mapped from orthophotos and Sentinel on the same day, 27 August 2019. Left: orthophoto from norgebilder.no. Right: Sentinel-2 image. Edit, manual edits; S2ed, Sentinel-2 with manual edits; ortho, manual digitised from orthophoto; snow, polygons classified as snow; S2aut, automatic outline classified from Sentinel-2. Note that the lakes are included in the automatic mapping. None of the lakes are now connected to the glacier. See Figure 1 for location. /Copernicus Sentinel data 2019/© Norgebilder.no/.

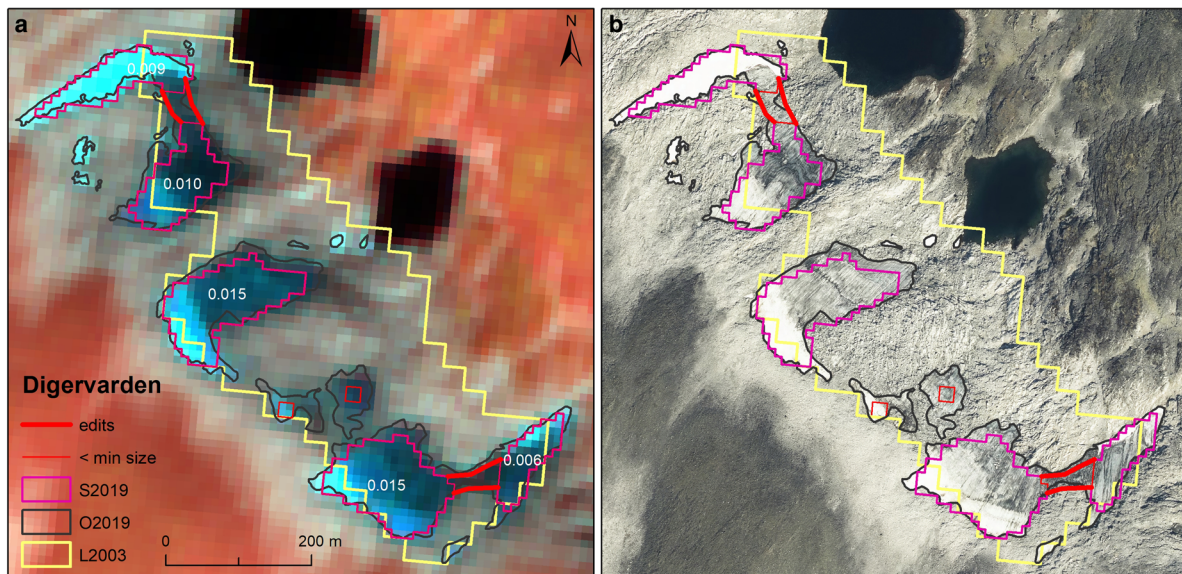


Fig. 10. Small ice patches mapped from Sentinel-2 (S2019) at Digervarden, Lesja, Innlandet county, compared to independent manual digitization from orthophotos taken the same day (O2019). (a) Sentinel-image from 27 August 2019 (false 11-8-4). (b) Orthophoto from the same day. The ice patches were mapped as one body (L2003) in the 1999–2006 inventory, and there included as a possible snowfield layer without any assigned ID./Copernicus Sentinel data 2019/© norgebilder.no/.

km² in 2018–2019, a reduction of 411 km² or 15.3%. All 36 glacier regions used in the 1999–2006 inventory (Andreassen and others, 2012; Winsvold and others, 2014) have a reduced glacier area, with the largest losses in the northernmost regions (Fig. S6). When only considering the glaciers mapped in the 1999–2006 inventory, the glacier area in northern Norway (regions 1–19) was reduced from 1170 to 910 km², a loss of 260 km² or –22%. The glacier area in southern Norway (regions 20–36) was reduced from 1522 to 1371 km², a loss of 151 km² or –10%. The largest

losses are observed in Svartisen East (55 km²), Svartisen West (39 km²) and Jotunheimen West (26 km²). It should be noted that the northern regions 4–19 have 1999–2006 mapping years 1999 and 2001, whereas the southern regions were mapped in 2002, 2003 and 2006, thus most of the changes in northern Norway are for a longer period. Looking at percentage change per year for all regions, the five regions with the most negative change per year are: 35 Hardangervidda, 18 Vefsn, 8 South Troms, 34 Hardangervidda and 32 Hallingskarvet, with changes

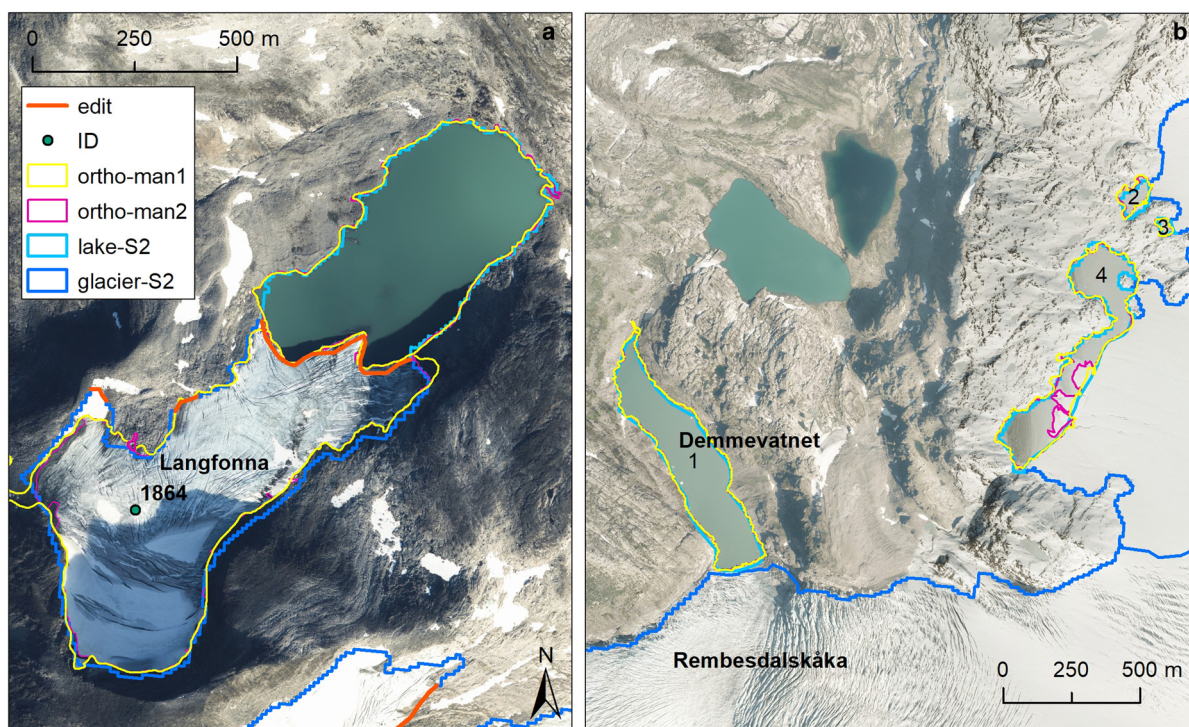


Fig. 11. (a) Glacier lakes Langfonna, Møre. (b) Glacier lakes at western part of Hardangerjøkulen (HAJ). See Figure 1 for location. Orthophotos from © norgeibilder.no are from (a) 27 August and (b) 26 July (left part) and 21 September 2019 (note the fresh snow).

Table 2. Lake area derived for a lake at Langfonna and several lakes at Hardangerjøkulen

Lake Area	S2 km ²	O-man1 km ²	O-man2 km ²	S2-man1 ΔA (%)	S2-man2 ΔA (%)
Langfonna	0.235	0.232	0.234	1.2	0.2
1 -Demme	0.144	0.146	0.142	-1.4	1.3
2	0.009	0.009	0.010	-8.1	-16.2
3	0.003	0.003	0.003	-3.8	-3.5
4	0.111	0.103	0.117	7.1	-6.0

S2: lake area mapped from Sentinel-2. O-man1 and O-man2: digitised manually from orthophotos. S2-man1 and S2-man2: differences (percentage) between lake areas derived from Sentinel-2 and from orthophotos. See Figure 11.

ranging from -3.2 to -3.0% a^{-1} . All these regions are characterised by small glaciers. The regions with the smallest negative changes are 25–27 Jostedalsbreen (South, Mid, North), 33 Hardangerjøkulen and 32 Folgefonna, with changes in the range between -0.27 and -0.62% a^{-1} . These regions include some of the largest glaciers in Norway.

Some of the glacier complexes have parts that are now detached from the main glacier, such as Gihstsejegna (Fig. 13b). The detached parts are not counted in the current area for the glacier complex, but as a separate unit. The detached glaciers are, however, included in the overall glacier area for Norway and in glacier change analyses. Furthermore, it should be noted that some of the disconnecting of glaciers in the new inventory is likely attributed to better spatial resolution of the Sentinel-2 imagery and availability of orthophotos as opposed to actual breakup of glaciers between the inventories. The ten largest glacier complexes have all shrunk since 1999–2006 (Table 4). When including the detached parts in the analysis to assess the overall glacier changes, a total reduction of 87 km^2 or 6.6% of the ten complexes is observed. The largest relative reduction is for Okstindbreen (0.7% a^{-1}), whereas Jostedalsbreen has been reduced the least in relative area (0.2% a^{-1}). Some of the individual tongues of Jostedalsbreen have retreated markedly, such as Bødalsbreen

($\sim 880\text{ m}$), Nigardsbreen ($\sim 650\text{ m}$), Austdalsbreen ($\sim 300\text{ m}$) and Tuftebreen ($\sim 200\text{ m}$) (Fig. 13a).

Looking at the change of individual glaciers for the 3143 glaciers mapped in 1999–2006 and 2018–19. As expected, there is more variability for the smallest glaciers (Fig. 14). When inspecting the glaciers and comparing them with the 1999–2006 outlines, it was clear that in many cases, the smallest glaciers were mapped differently due to the higher resolution of Sentinel-2 (10 m) than Landsat (30 m). Moreover, the changes in ice divides and topology for some of the units give changes that are due more to methodology than actual glacier changes. Paul and others (2020) decided not to compare glacier by glacier from their 2003 Landsat inventory to their 2015 Sentinel-2 inventory for the European Alps as glacier-specific comparison was difficult due to differences in interpretation and a different location of the ice divides. Results must be interpreted with care for individual glaciers as the ruleset for glacier identification changes with different resolution of the datasets. We recommend checking orthophotos and the satellite imagery, as well as the glacier outlines from both inventories.

5.3. Glacier lakes

In total, we mapped 455 ice-marginal lakes in direct contact with the glaciers at the time of mapping. The surface areas of the lakes range in size from 0.00042 to 38.5 km^2 (Storglomvatnet, Svartisen) with a total of 90.6 km^2 and mean (median) of 0.20 km^2 (0.15 km^2). Of the lakes, 360 lakes with a total area of 10.1 km^2 were newly formed or not mapped in the glacier lake inventory from 1999 to 2006 (Andreassen and Winsvold, 2013). We mapped nearly 200 lakes that were not included in the 2018 product, mainly due to inclusion of lakes associated with glaciers in the size category 0.05 – 0.25 km^2 that were not included in the 2018 mapping (Nagy and Andreassen, 2019; Andreassen and others, 2021).

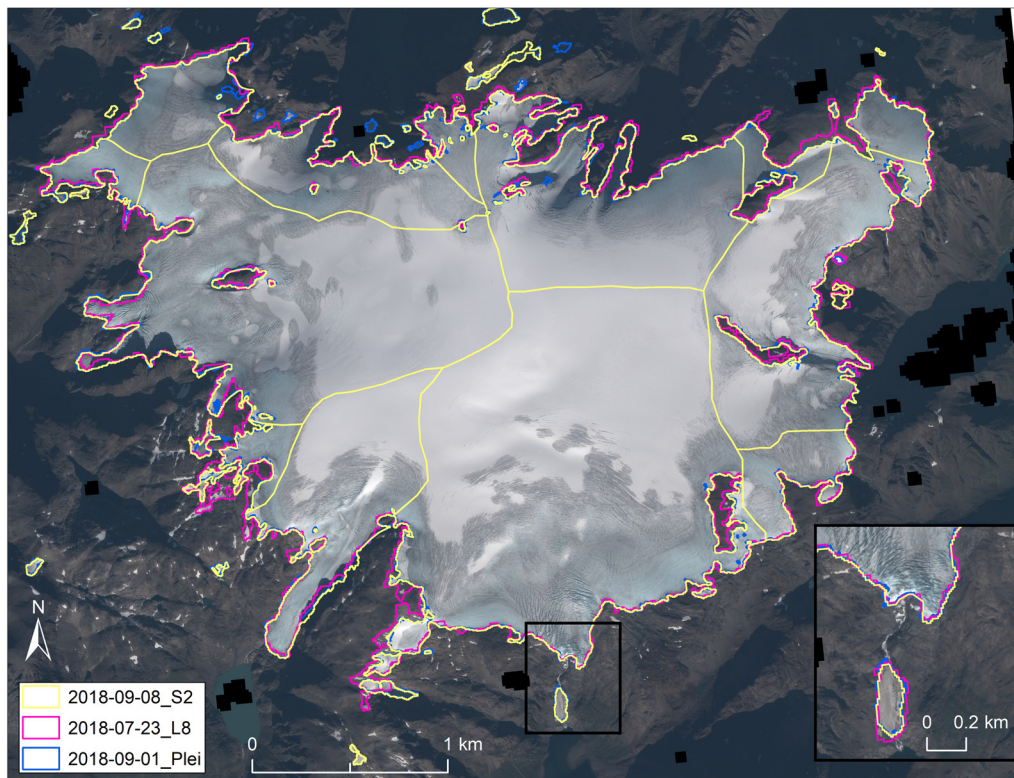


Fig. 12. Øksfjordjøkelen in Finnmark mapped manually from Pléiades orthoimage and semi-automatically from Sentinel-2 and Landsat 8 images from 2018. Inset shows the lower part of the outlet Isfjordjøkelen (ID 47) and the regenerated glacier Nerisen (ID 48). Background is Pléiades image shown in colour at 2 m resolution. The black pixels represent unmatched areas in the orthoimage. /Pléiades © CNES 2019, Distribution Airbus DS/.

Table 3. Mapped glaciers and ice patches included in the 2018–19 inventory derived from Sentinel-2 per size class

Glacier Size class	South		North		Norway		Total % of area
	Area (km ²)	<i>n</i>	Area (km ²)	<i>n</i>	Total	<i>n</i>	
>5 km ²	688.3	67	393.3	29	1081.6	96	46.5
1–5 km ²	427.6	197	302.3	139	729.8	336	31.3
0.5–1 km ²	95.5	139	67.5	95	163.1	234	7.0
0.1–0.5 km ²	119.0	532	105.4	480	224.9	1012	9.7
0.05–0.1 km ²	29.6	421	24.0	347	53.5	768	2.3
0.01–0.05 km ²	35.8	1461	32.0	1353	68.0	2814	2.9
<0.01 km ²	4.1	766	4.1	710	8.3	1476	0.4
Total	1399.9	3583	928.5	3153	2328.4	6736	100

A, area; *n*, number. The glaciers are divided into units, e.g. Jostedalsbreen as more than 80 units.

In our study, large lakes that have a clear glacier-ice interface were easy to identify and distinguish from the glaciers, whereas smaller and shallow lakes were more difficult to identify. Comparison with glacier lake and glacier outlines from 1999 to 2006 revealed a clear growth of many glacier lakes, formation of new lakes and some lakes no longer in contact with the glaciers (Fig. 15). For some glaciers, existing lakes have grown as glaciers have retreated such as Glacier ID 2532, a detached glacier that was connected to Spørteggbreen in the 1960s (Fig. 15a). Here images from 2006, 2014 and 2019 clearly show the retreat of the glaciers. While the two largest lakes were already present in 2006, new lakes have formed along the perimeter as the glacier has retreated (Fig. 15a). At the ice cap Hardangerjøkulen, many lakes have formed along the relatively flat western part that has been exposed as the ice has retreated (Fig. 15b). Vetlefjordsbreen from Jostefonni was calving in the lake in 2006 and the lake has continued to grow since then. The glacier has now retreated upslope

and is no longer connected to the lake (Fig. 15c). Austerdalsisen from Østre Svartisen was also connected to the lake in the last inventory dating back to 1999 and has in recent years retreated from the lake. The distance to the lake was 150–200 m in 2018 (Fig. 15d). The glacier lakes of Vetlefjordsbreen and Austerdalsisen were therefore not included in the 2018–19 dataset but are found in the historical glacier lake outline datasets. It was also clear that glacier lakes grew from 2018 to 2019 in southern Norway, by comparing the 2018 product with the updated product. Thus, Sentinel-2 can be used to show glacier lake growth at an annual scale. Some of the glacier lakes are dammed by the glacier or by moraines and are occasionally partly or fully drained. One of the glacier-dammed lakes, Demmevatnet at Rembesdalskåka, drained prior to 27 August 2019, the time of the mapping of Hardangerjøkulen. Here we included the lake perimeter from 4 August 2019 (Fig. S3).

6. Discussion

6.1. On what to include in a glacier inventory

It can be challenging to decide what to include and exclude in an inventory. We wanted to include the parts containing ice, not seasonal or pure snowfields. In Norway, snowfields can be persistent and checking the available orthophotos revealed that many of them are long lasting and likely change little over time. For example, orthophotos and Landsat images from 2006 revealed minimal snow conditions in the Jostedalsbreen and Møre regions compared to more recent orthophotos and satellite images of 2019. Several years with mass surplus in the last decade (Andreassen and others, 2020b) have resulted in transient growth of snowfields as well as glaciers. Snow conditions do not only depend on the current year but also on perennial snowfields that survive several years.

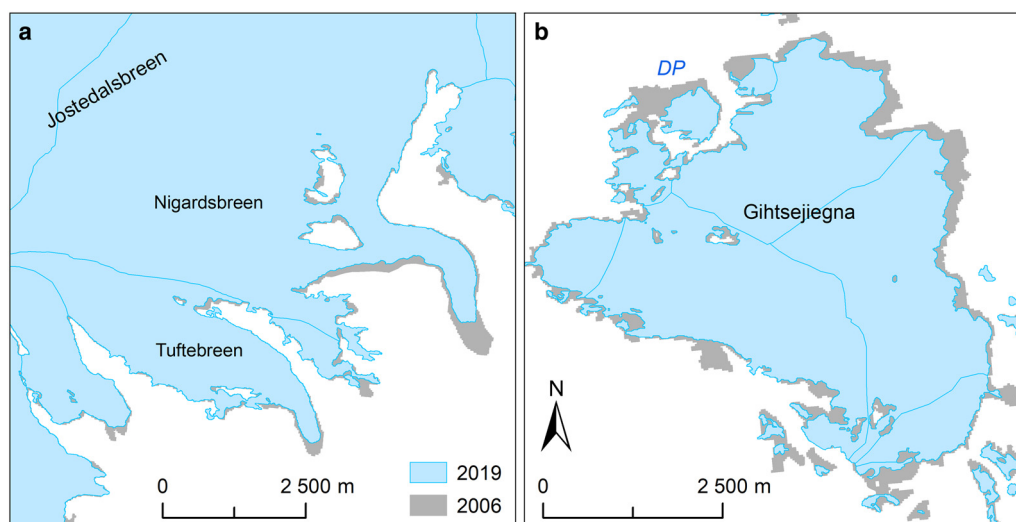


Fig. 13. Glacier changes comparing 2018–19 with 1999–2006 for (a) Nigardsbreen and Tuftebreen, outlets of Jostedalbreen, (b) Gihlsejiegna. DP, detached parts from main glacier since 1999–2006. The individual mapping years are given. Note that map scale differs. The grey colour shows where the glaciers have shrunk from the previous to the current inventory. See Figure 1 for location.

Table 4. List of the ten largest glacier complexes in Norway and their change since the 1999–2006 inventory

No.	Glacier Name	Years (n)	Date (date)	1999/2006		2018/2019			1999/2006–2018/2019		
				Area (km ²)	Date (date)	Date (date)	Area (km ²)	Area* (km ²)	Area change (km ²)	Area change (%)	Area change (% a ⁻¹)
1	Jostedalbreen	13	2006-09-16	473.8	2019-08-27	458.1	459.7	-14.0	-3.0	-0.23	
2	Vestre Svartisen	19	1999-09-07	218.1	2018-09-08	190.2	197.2	-20.9	-9.6	-0.51	
3	Søndre Folgefonna	17	2002-09-13	164.2	2019-08-27	153.8	154.1	-10.1	-6.2	-0.36	
4	Østre Svartisen	19	1999-09-07	147.7	2018-09-08	125.1	132.0	-15.7	-10.6	-0.56	
5	Blåmannsisen	19	1999-09-07	87.3	2018-09-08	80.8	81.0	-6.2	-7.1	-0.37	
6	Hardangerjøkulen	16	2003-08-09	71.3	2019-08-27	64.1	64.9	-6.4	-8.9	-0.56	
7	Myklebustbreen	13	2006-09-16	47.7	2019-08-27	45.1	45.1	-2.5	-5.3	-0.41	
8	Okstindbreen	19	1999-09-07	53.6	2018-09-08	36.9	46.5	-7.1	-13.3	-0.70	
9	Øksfjordjøkelen	12	2006-08-28	38.6	2018-09-08	36.2	36.2	-2.4	-6.2	-0.51	
10	Nordre Folgefonna	17	2002-09-13	26.4	2019-08-27	23.9	24.0	-2.5	-9.3	-0.55	
10	Sum			1328.6		1214.2	1240.8	-87.9	-6.6		

Area is the area of the complex, and area* includes parts disconnected in 2018–19 that were included in the 1999–2006 outlines. Glacier changes are calculated from the area of 1999–2006 and the area* of 2018–19.

We mapped more smaller ice bodies than in the 1999–2006 inventory. An increase in the number of glaciers was also the case for the 1999–2006 inventory compared to previous inventories based on analogue aerial photography, with the explanation that automatic mapping typically includes more glaciers than manual digitising (Andreassen and others, 2012). For example, in central Troms and Finnmark county, Leigh and others (2019) found more glaciers using a semi-automated approach with cross-checking on 0.25 m aerial imagery, including 78 newly identified and mapped ice bodies in their analysis of the glacier area. Similarly, in the latest glacier inventory of the European Alps using Sentinel-2, Paul and others (2020) noted that many very small glaciers that are now included were not mapped or were mapped too small in the prior Alps-wide inventory (Paul and others, 2011). The 2020 European Alps glacier inventory included 4395 units larger than 0.01 km² (Paul and others, 2020), while the 2011 inventory included 3770 units larger than 0.01 km² (Paul and others, 2011).

Sentinel-2 images can be used to observe ice and crevasses for larger glaciers, but this is more difficult on smaller bodies. A sub-region of 161 km² in Møre (Fig. 1) was chosen to compare differences between the classification we used for 2018–19 and the classification according to Leigh and others (2019). Author 1

had controlled the automatically mapped polygons using Sentinel-2 imagery and orthophotos for the final 2018–19 outlines, while author 2 scored the polygons independently according to Table S3 using the orthophotos (Fig. 16). Results showed that for the 58 polygons, nine of them were classified as snow by author 2, representing an area of 0.101 km². On the other hand, author 2 scored 20 of the classified snow polygons as ice patches and PSFs amounting to 0.004 and 0.062 km², respectively, in total 0.066 km². Moreover, author 2 also suggested to score many of the smaller ice patches as possible glaciers based on orthophotos, where there appeared to be an indication of crevassing and/or deformation of debris banding. Deformed debris bands may be remnants of former glacier flow, with the present-day ice body having shrunk to the point at which it retains their presence without any glacier motion.

Furthermore, there is potential for very small glaciers (e.g. smaller than 0.5 km²) to persist in isolated topographic niches, with a high proportion of debris cover and/or extensive intense shading (e.g. Capt and others, 2016; De Marco and others, 2020). These glaciers gain mass from wind-blown and avalanche snow (Helfricht and others, 2015), gain mass and insulation from rock wall debris input (Bosson and Lambiel, 2016), are protected from solar radiation by relief (Olson and Rupper, 2019) and can

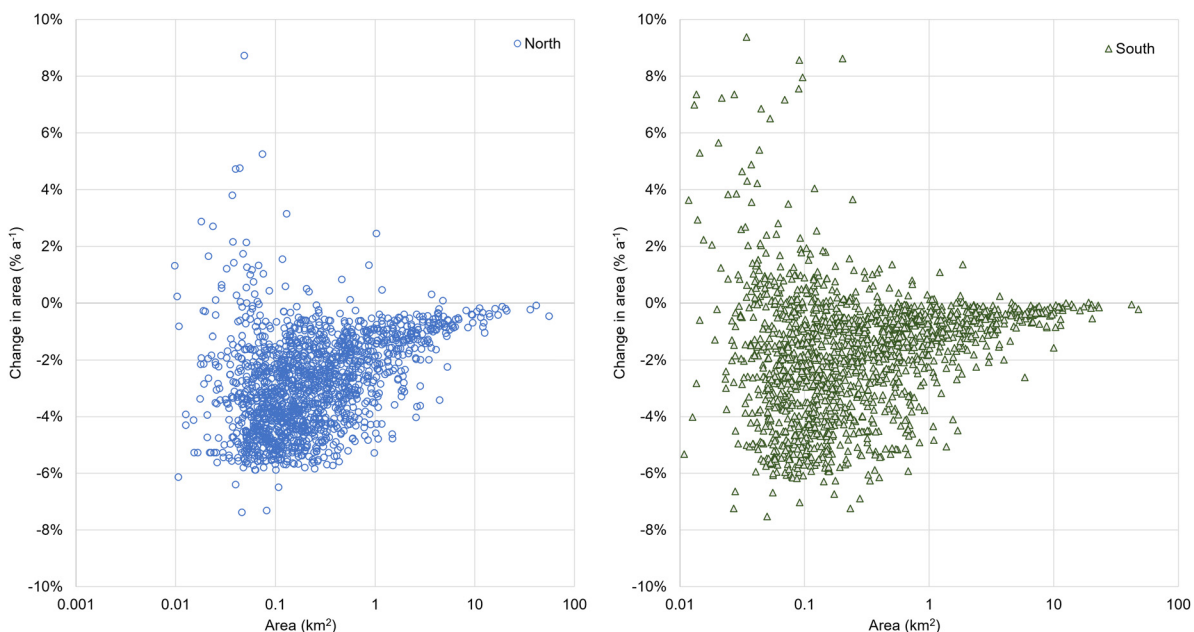


Fig. 14. Glacier change in $\% a^{-1}$ from 1999–2006 to 2018–19 for the 3143 glaciers mapped in 1999–2006 divided into (a) North and (b) South. Note that area scale is logarithmic. Area size is the original size in 1999–2006.

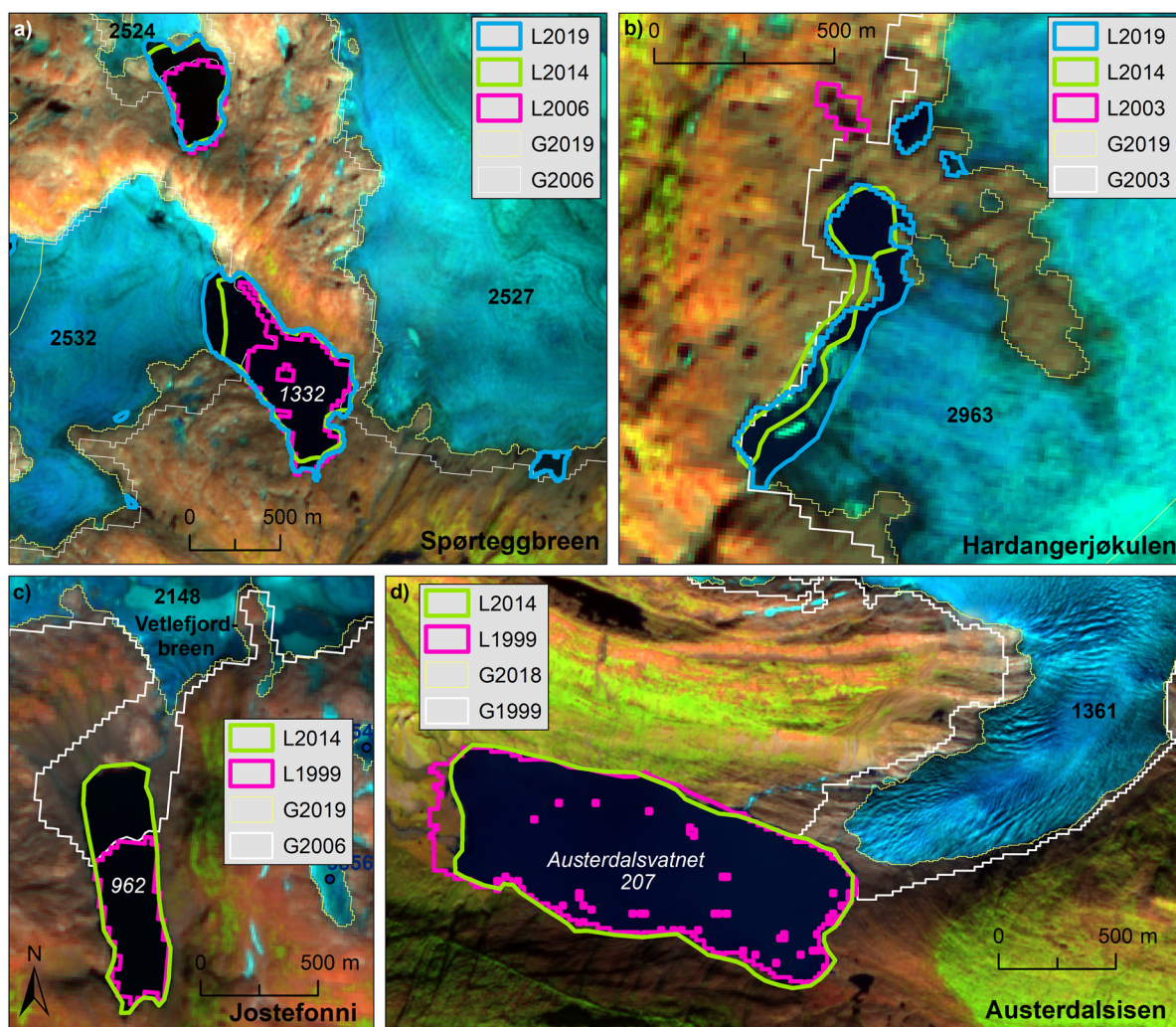


Fig. 15. Subsets of Sentinel-2 scenes (false 11-8-4) (a), (b) and (c) are scenes from 27 August 2019, (d) is a scene from 8 September 2018 showing glacier retreat, lake formation and growth between the previous 1999–2006 inventory and the current 2018–19 inventory. Lakes derived from Landsat images of 2014 are also shown. G, glacier outline; L, glacier lake outline and year denotes year of Sentinel-2 or Landsat image. (a) Part of Spørteggbreen (2527 and 2524) and detached patch 2532. (b) Part of western Hardangerjøkulen (2963) north of Rembesdalskåka. (c) Vetlefjordbreen (2148), part of Jostefonni where the glacier lake has grown, and the glacier has retreated out of the lake. (d) Austerdalsisen, outlet of Østre Svartisen, where the glacier was connected to the lake but now retreated upslope and is no longer attached. Elevations of lakes in white italic from norgeskart.no. Glacier IDs in black. /Copernicus Sentinel data./



Fig. 16. Illustration of part of an area in Møre where the scoring system was tested on an orthophoto to classify glaciers, ice and snow using Sentinel-2. The inset shows the total area used for testing the scoring system and the extent of the part shown in detail. See Figure 1 for location. The green and yellow outlines reveal differences between the classification; green shows where snow was interpreted as ‘possible’ glaciers/ice patches and yellow where a classified ice patch was interpreted as snow using the scoring system. The filled polygons show where orthophoto scoring and mapping suggested inclusion of more possible glaciers/ice patches (ortho – mP) and more edits of the existing polygons (ortho – mE) in the 2018–19 inventory. Background orthophoto of 27 August 2019 from ©norgebilder.no.

be strongly influenced by permafrost conditions (Etzelmüller and Hagen, 2005). Very small glaciers can form at the base of rock walls, within recesses on steep valley sides, and/or impounded by large moraines or rock lips. Such glaciers are more likely to be missed or discarded in regional glacier inventories, especially those that rely on an automated component that is known to be more susceptible to miss shaded/debris-covered ice or which excludes potential false positives based on slope profiles. However, we are confident that we did not miss many ice bodies $>0.1 \text{ km}^2$ with the thorough inspection we did for this inventory.

Recently, Leigh and others (2019, 2020) identified several undocumented snow/ice-bodies in northern Norway that exist in heavily shaded niches, some of which are also debris covered. For example, Figure 17 shows two units that have not been recorded in any prior inventory or map: a $\sim 0.02 \text{ km}^2$ unit situated within a niche on a rock wall, $\sim 140 \text{ m}$ above glacier 123 (Figs 17a–e) and a $\sim 0.03 \text{ km}^2$ partially debris-covered unit in an alcove below a rock wall and impounded by a large moraine (Figs 17f–i). On the Sentinel-2 imagery, it is difficult to discern the units or differentiate them from a snow patch (Figs 17e, i), and even on the aerial imagery from 2016 (Figs 17d, h), persistent snow cover prevents any identification of glacier ice. It has only been possible to determine the likely nature/origin of these units by viewing them in the field where oblique observations at a time with minimal snow cover (September) allow for ice, with debris banding to be detected (Figs 17b, g). It is not possible to obtain ground photographs for all ice/snow bodies across Norway. Therefore, it is highly likely that current limitations will inevitably mean some potential glaciers will be misclassified or remain undocumented.

6.2. Uncertainties in identifying and mapping very small glaciers on different image sources

In the central regions of Troms and Finnmark county (formerly classified as northern Troms and western Finnmark), Leigh and others (2020) used a semi-automated mapping approach on Landsat imagery from 2018 to map the glaciers and assess glacier changes. This is the same year as we used for our Sentinel-2 mapping in this region. In total, they mapped 252 glaciers on pansharpened Landsat-8 OLI imagery (15 m resolution; image date 28 July 2018) with a total glacierised area of 66.4 km^2 . Of the 252 glacier units mapped by Leigh and others (2020), 202 of these

(equating to 65.29 km^2) align with units mapped in this study using Sentinel-2 imagery (10 m resolution; equating to 61.52 km^2), while the remaining 50 units (equating to 1.13 km^2) were not included in the Sentinel-2 imagery. Furthermore, mapping conducted with the Sentinel-2 imagery identified an additional 139 units (equating to 1.38 km^2) not mapped using Landsat-8 imagery. The differences in which glaciers were mapped in our inventory compared to Leigh and others (2019) highlight the difficulty of identifying and mapping very small glaciers ($<0.02 \text{ km}^2$) from different image sources and using slightly different techniques.

Differences between our Sentinel-2 based glacier outlines and the aligned glacier units from the Landsat-8 based outlines can result in both larger and smaller units. For example, glacier ID 60 was mapped as 0.06 km^2 on the Sentinel-2 imagery compared to 0.11 km^2 on the Landsat-8 imagery ($\sim 0.05 \text{ km}^2$ or 83% larger in area), whereas glacier ID 128 was mapped as 0.49 km^2 on the Sentinel-2 imagery compared to 0.38 km^2 on the Landsat-8 imagery (a ~ 0.12 or 29% smaller area; Fig. 18). On average, however, the Sentinel-2 derived outlines are $\sim 0.02 \text{ km}^2$ smaller than those mapped from Landsat-8 imagery, giving a smaller total area of the overlapping glaciers of 3.77 km^2 (6%). The differences between the Sentinel-2 and Landsat-8 derived outlines for glaciers in valleys or cirques were smallest, even when considering the associated difficulties in mapping these units (e.g. heavy shading, supraglacial debris). The greatest differences were found for the glaciers located on elevated plateaus, such as glacier ID 120, which when mapped using Sentinel-2 imagery was definable as three separate units equating to a total area of $\sim 0.08 \text{ km}^2$. When mapped using Landsat-8 imagery it was depicted as one unit with an area of $\sim 0.2 \text{ km}^2$, representing an approximate 150% (0.12 km^2) increase in the mapped glacier area. Mapping glaciers accurately is difficult at higher elevations, particularly owing to the prevalence of late-lying snow that can mask glacier boundaries.

There were also some differences associated with unit classification, whereby individual glacier/ice units are assigned specific classification (see Section 4.2, Table S3) based upon visual inspection of key glacial indicators (Leigh and others, 2019). The greatest differences in unit classification were found on those units smaller than 0.1 km^2 . Figure S7 provides an example of a previously unmapped body that has subsequently been mapped on Sentinel-2 imagery with an area of 0.03 km^2 (this study) and on

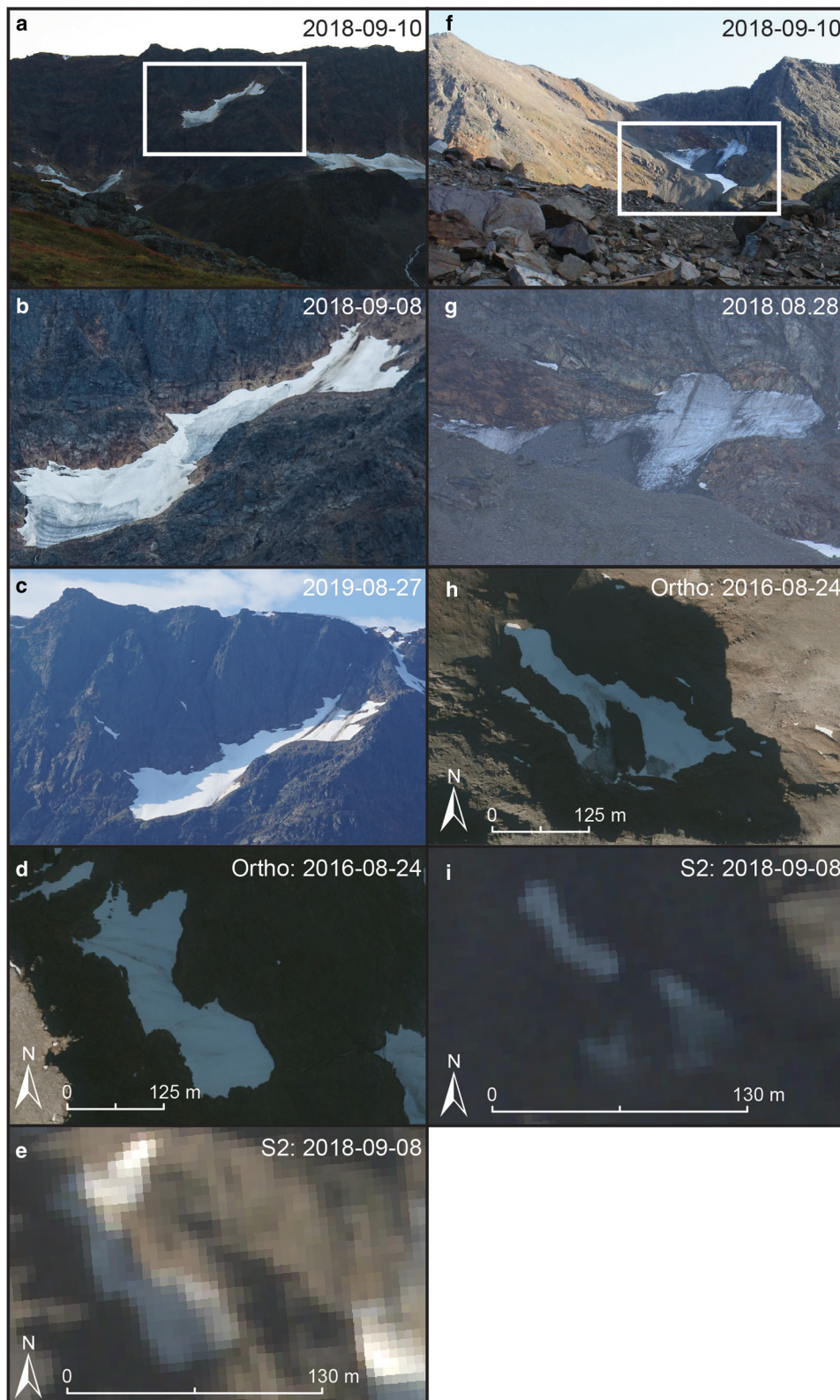


Fig. 17. Two very small ice bodies in the Kåfjord Alps (Troms and Finnmark county) first identified on high-resolution aerial imagery and subsequently viewed in the field. (a–e) A small (choose to refer to this as either ice/snow unit or glacier) within a niche on a rock wall above glacier 123; (a) oblique field photograph showing the ice/snow unit within the white rectangle, (b) zoomed in photograph showing bare ice, debris banding and a small ridge at its front, (c) a year later but with complete snow cover, (d) the unit from aerial imagery, (e) the unit from Sentinel-2 imagery. (f–i) A small glacier in an alcove below a steep rock wall, impounded by a large moraine, and partially debris covered; (f) oblique field photograph showing the ice/snow unit within the white rectangle, (g) a zoomed in photograph showing bare ice, some debris banding and debris cover, (h) the unit from aerial imagery, (i) the unit from Sentinel-2 imagery. /Copernicus Sentinel data 2018/© norgebilder.no/.

Landsat-8 imagery with an area of 0.05 km^2 (Leigh and others, 2020). Following the glacier scoring system, Leigh and others (2020) classified this new unit as a certain glacier based on the

presence of multiple visual clues in the 2006 imagery (e.g. deformation of debris banding, evidence of multiple debris bands, bare ice, moraines in the recently deglaciated foreland).

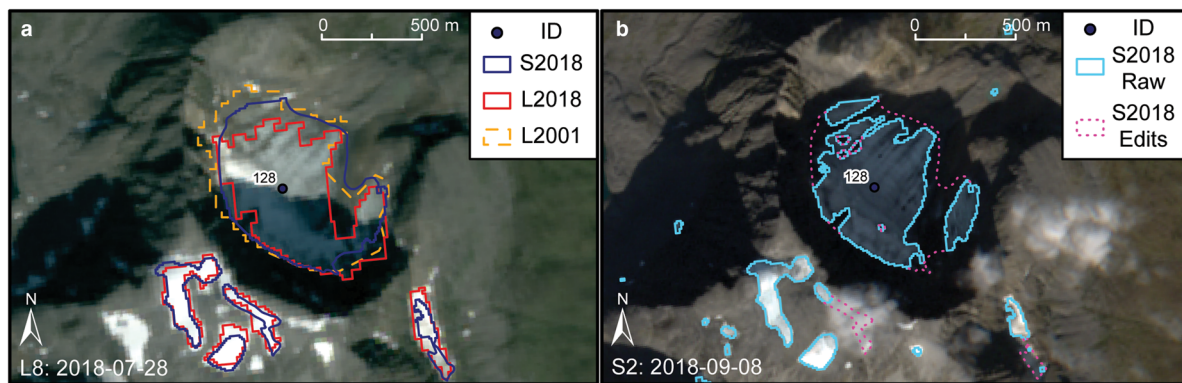


Fig. 18. Edited 2018 Sentinel-2 outlines (S2018), original 2018 Landsat 8 outlines (L2018; Leigh and others, 2020), and original 2001 Landsat 7 outlines (L2001; Andreassen and others, 2012); (b) unedited glacier outlines (S2018 Raw) and manual edits (S2018 Edits). Note: in (a) and (b) Landsat 8 (L8) and Sentinel-2 (S2) imagery are both shown in natural colours. /Copernicus Sentinel data 2018/.

However, for the purpose of this study it was only classified as an ice patch/PSF. When such units are cross-checked on high-resolution colour orthophotos, interpretation and distinction between glacier ice vs remnant glacier ice vs non-glacial ice patches remains challenging, especially when there are unfavourable snow conditions (e.g. Figs S7d, e).

While there are undoubtedly differences in associated glacier area resulting from varying image resolution, differences also result from image capture date and time as extent and intensity of shading will change throughout the year and day. The mapping date of the Landsat-8 imagery was earlier in the melt season (28 July 2018) than the Sentinel-2 imagery (8 September 2018). The prevalence of late-lying snow has the potential to mask glacier boundaries, making the unit appear larger than it really is (Fig. 18). The smaller total area (6%) in the overlapping area in our Sentinel-2 mapping compared to the Landsat-8 mapping illustrates how results can differ within the same year. The end of July is probably a bit too early for optimal glacier mapping and it is in general better to use images from later in the season. We mainly used dates from the 1 or 8 September 2018 for northern Norway and 27 August 2019 for southern Norway for our 2018–19 inventory. Earlier scenes from 4 and 15 August 2019 had to be used for some glaciers in southern Norway due to clouds (Fig. 2). Thus, a compromise of image capture date may be needed to secure imagery from the necessary year, at the risk of overestimating the glacier area. Substantial cloud cover over the coastal areas of Norway results in a decreased availability of appropriate satellite imagery (e.g. Winsvold and others, 2014). While Sentinel-2 provides a better temporal resolution (5-day repeat cycle, more frequent at the higher altitudes), Landsat-8 (16-day repeat cycle) is still valuable for glacier change detection.

Comparing the four largest glacier composites in the overlapping Landsat-8 and Sentinel-2 sample for Troms and Finnmark county shows that all glaciers are larger in Landsat-8 mapping than in the Sentinel-2 mapping (Fig. S4). The four ice caps had a total area of 49.9 km² in Landsat-8 and 48.3 km² in Sentinel-2, thus the glacier area was 3.3% larger from Landsat-8. The area derived from outlines digitised from Pléiades imagery for two of the glaciers, Langfjordjøkelen and Øksfjordjøkelen, as described in Section 4.5.5 was smaller (Table 5, Fig. 12, Fig. S4). Compared to Sentinel-2 (36.3 km²), the Pléiades area was –1.2% smaller (35.9 km²) and the Landsat area was 2.5% larger (37.3 km²). Again, the Landsat-8 mapping was conducted on an earlier image and a true comparison would need a closer time gap between acquisition dates. The agreement in mapped area between the Pléiades orthoimage and Sentinel-2 imagery shows

that Sentinel-2 can be used for accurate glacier mapping for clean ice with limited shadowing.

6.3. Uncertainty estimates and validation

In the 1999–2006 inventory, an overall uncertainty of 3% was estimated, using validation data in a subset of glaciers in one region. The uncertainties in estimating the area of glaciers and glacier lakes from the new 2018–19 inventories have been assessed in this study using orthophotos and Pléiades orthoimages and testing out band ratio and band 2 thresholds. This revealed that the relative uncertainty increased with decreasing glacier size. An overall uncertainty between <1 and 3% can be expected, but individual uncertainties can be much larger for the smallest glaciers. Although we had good validation datasets from Pléiades and orthophotos, these were also partly challenging to analyse due to dark ice in some parts (Figs 7, 8). To assess the real accuracy, we need to compare our estimates with field measurements. Even with validation data as we have there, we do not have ground truthing. Our manual digitisation revealed that both the number and area of mapped glaciers varied between the digitisers. Still, results showed good overall agreement and revealed that the Sentinel-2 band ratio-based mapping worked well, except for parts in shadow or with debris where the uncertainties are larger. We conclude that for clean ice, the Sentinel-2 semi-automated mapping has an accuracy comparable to manual digitising from high-resolution data.

Another common method is to assess the uncertainty using the buffer method, by applying a negative or positive buffer around glacier outlines. This also reflects the sensitivity of the result. We assessed this impact by applying a negative or positive buffer around glacier outlines. Assuming an uncertainty along the perimeter corresponding to the Sentinel-2 10 m pixel size, we created buffers of ± 5 and ± 10 m around the glacier and glacier lake polygons. For all the glacier polygons, a ± 5 m buffer resulted in a change in area of $\pm 3.1\%$, increasing (decreasing) the glacier area to 2401 (2257) km² (Table 6). A ± 10 m buffer nearly doubles the area change to $\pm 6\%$. Looking at Jostedalbreen, the largest glacier complex, the impact of a ± 5 and ± 10 m buffer was an area change of ± 1.1 and $\pm 2.3\%$, respectively. For the ten largest glaciers, the impact of a ± 5 and ± 10 m buffer was an area change of 1.0 and $\pm 1.9\%$, respectively. For rounder glaciers, the impact will be smaller; for elongated glaciers, the impact will be larger. The smallest glaciers have the largest relative changes in area, e.g. for a small ice patch like Juvfonne (0.1 km²), the impact of a ± 5 and ± 10 m buffer was ± 9 and $\pm 18\%$, respectively. The Juvfonne area was derived

Table 5. Comparison between glacier outlines of the largest four glaciers in the central region of the Troms and Finnmark county using three different imagery types with different image capture dates in 2018: Sentinel-2 (S2) (10 m) of 8 September, pansharpened Landsat-8 (L8) (15 m resolution) of 28 July, and Pléiades (P) (0.5–2 m resolution)

Glacier Date	Area (km ²)		
	S2 8 Sep	L8 28 July	P 1 Sep
Svartfjelljøkelen	3.7	3.9	
Øksfjordjøkelen	36.3	37.3	35.9
Langfjordjøkelen	6.4	6.8	6.2
Noammerjehkki	1.8	2.0	
Total (all)	48.3	49.9	
Total (Øks + Lang)	42.8	44.0	42.1

Note that for the Sentinel-2 imagery-based outlines for Landfjordjøkelen, the Pléiades image and outlines were compared when deciding the ratio and as such, these outlines are not independent. See Figure 12 for the Pléiades imagery of Øksfjordjøkelen.

from Sentinel-2 on 4 August 2019 (not 27 August due to clouds) and is 0.106 km², whereas the outlines derived from the orthophoto from 26 August 2019 give an area of 0.087 km² (Fig. 19). This was indeed the same as an 18% reduction, but part of the difference is due to melting around the perimeter in the 22 days from the Sentinel-2 acquisition compared to the orthophoto acquisition. Snowy parts in the southwestern part were included in the Sentinel-2 automatic outline, but not in the manual digitisation from the orthophoto due to melting (Fig. 19). For this thin ice patch, the variations around the perimeter are large from year to year and during the melt season (Ødegård and others, 2017; Andreassen and others, 2020a).

In this study, we validated our S2-mapping to manual digitisations from orthophotos and orthoimages, tested the sensitivity of different thresholds and tested the sensitivity by applying buffers. A summary of these tests shows that for glaciers larger than 0.3 km², relative area differences are within 7% (Table 7). The validation data reveal larger relative differences for smaller glaciers, similar to what we see for the buffer method (Table 6). The result for the smallest glaciers was very sensitive to manual edits and snow conditions at the time of mapping. The S2-areas were both smaller and larger than the area derived from the validation data. For groups of glaciers, the relative area differences were smaller. Based on our validation results, we find them in a line with a ± 5 m buffer for all of Norway. Thus, we estimate the total uncertainty in the glacier area of Norway to be $\pm 3\%$ or 70 km². The reduction in glacier area from 1999–2006 to 2018–19 ranges between 364 and 411 km² or 14 and 15%, depending on whether we compared the total area from 2018 to 2019 with the total area from 1999 to 2006 (13.5%), the total area from 2018 to 2019 with 1999–2006 including the PSF (14.3%), or only glaciers mapped both in 2018–19 and 1999–2006 (15.3%). The reduction in area was for all samples larger than the uncertainty in the total areas of both 1999–2006 (3%, 81 km²) and 2018–19 (3%, 70 km²).

The accuracy of the glacier lake mapping was tested for a sample of five lakes and revealed relative differences within $\pm 1.5\%$ for two of the lakes >0.1 km². For a lake that had floating ice and the two smallest lakes, a relative difference of up to 16% was found. The accuracy of the semi-automated glacier lake mapping using NDWI for the 2018 lake outlines was also tested using manual digitisations of nine lakes from orthophotos from norgebilder.no and revealed a 4% accuracy (Nagy and Andreassen, 2019). The impact of different image acquisition dates on lake area was also assessed for a subset of seven lakes around Hardangerjøkulen over the period 13 July–3 September 2018, where snow cover and terrain-induced shadowing varied. The differences between the smallest and largest area of each lake ranged from 1.5 to 6.2%

Table 6. Sensitivity of buffer of size ± 5 and ± 10 m around the glacier polygons on the total area in % for all of Norway and a selection of the ten largest and some different sizes

Sample	Buffer size (m) km ²	5 m	–5 m	10 m	–10 m
		Δ %	Δ %	Δ %	Δ %
All glaciers	2328	3.1	–3.1	6.0	–5.9
10 largest	1214	1.0	–1.0	1.9	–1.9
Jostedalbreen	458.1	1.1	–1.1	2.3	–2.1
Blåmannsisen	80.8	0.8	–0.8	1.5	–1.5
Spørteggbreen	21.6	1.3	–1.3	2.5	–2.5
Steindalsbreen	4.39	2.4	–2.4	4.7	–4.7
Trollkyrkjebreen	0.856	3.1	–3.1	6.0	–5.9
Juvfonne	0.106	9.4	–9.2	18.3	–17.6
Kringsollfonna	0.023	28.5	–23.9	54.3	–47.8

Δ – Difference. See Figure 1 for location of glaciers.

(Nagy and Andreassen, 2019). From our findings, we estimate an accuracy of the glacier lake mapping within 3% for glacier lakes >0.1 km², except for glacier-lake interfaces with floating ice.

7. Conclusions

In this study, we used Sentinel-2 images from 2018 (northern Norway) and 2019 (southern Norway) to produce an updated dataset of glacier and ice-marginal lake outlines. We validated our glacier outline and glacier lake mapping with aerial orthophotos (0.25 m resolution) and Pléiades satellite orthoimages (0.5–2 m resolution) and tested the sensitivity by creating buffers around the glacier perimeter (Table 7). Overall, we estimated the accuracy within 3% for the overall glacier and glacier lake datasets. For the smallest ice or lake bodies, relative uncertainties were larger. A total of 60% (1400 km²) of the glacier area is in southern Norway and 40% (928 km²) is in northern Norway. The total glacier area is now 2328 ± 70 km², a reduction in glacier area by 15% when comparing only the glaciers mapped in the previous inventory 1999–2006. The 10 largest glacier complexes accounted for 1214 km² (52%) of the total area and have been reduced by 6.6% since 1999–2006. The area reduction has been largest in northern Norway (22%), compared to southern Norway (10%), but it should be noted that the period between inventories was larger for northern Norway. The 36 glacier regions have decreased in area ranging from -3 to -0.03% a⁻¹. In Norway, the regions with the largest percentage changes were dominated by small glaciers, and the regions with smallest percentage changes were dominated by the largest glaciers.

In total, over 2000 small glaciers and ice patches totalling 37 km² were mapped in this new 2018–19 dataset that were not included in the previous 1999–2006 glacier inventory. This was in part due to the higher resolution of Sentinel-2 (10 m) than Landsat (30 m), which was used for the previous inventory. All glacier bodies were carefully inspected using Sentinel-2 images, orthophotos and topographic maps. It is, however, noted that some smaller units (<0.1 km²) and parts of glaciers may still have been missed or excluded due to snow conditions, clouds, cast shadow, debris cover or misinterpretations. Some large bodies (>0.1 km²) classified as snow and not included in the 2018–19 inventory may have ice content. We applied manual edits to correct for glacier lake interfaces, debris cover, heavy shading and sometimes to detach snow patches. The manual editing needed to detach glacier lakes was used to produce an updated glacier lake outline dataset for 2018–2019 to match the new 2018–19 glacier outlines. We mapped 455 ice-marginal lakes that appeared to be in direct contact with the glaciers at the time of mapping, whereof 360 were new since the lake inventory from 1999 to 2006.

Table 7. Summary of validation and sensitivity tests and other comparisons in this study

Test	Region	Source	Outcome	Section
Band ratio thresholds, 1 glacier (0.4 km ²)	Jotunheimen, Gråsusnippen	S2	Using 2.4 as threshold T1 instead of 2.0 would reduce A by 0.016 km ² , or 4%	4.5.1 Figure 8
Manual digitisation, 15 glaciers (19.5 km ²)	Jotunheimen	S2, O	S2 total A 0.31% smaller than O. 10 (6) glaciers >0.1 (0.3) km ² , amounting to 99.2% (96.4) of the area, within ±4%	4.5.1 Figure 7, 8
Manual digitisation (2 dig), 49 glaciers, (40.6 km ²)	Jotunheimen	S2, P	S2 total A 0.78% smaller or 0.28% larger than P. Differences in which of the smallest glaciers included by digitiser. All glaciers >0.3 km ² within ±6%	4.5.1 Figure 4, 6, 7, 8
Manual digitisation, 3 glaciers (1.5 km ²)	Snøhetta	S2, O	S2 A 2.0% smaller than O. Without manual corrections of S2, S2 A 9.5% smaller. Two glaciers >0.3 km ² within ±6%	4.5.2 Table 1 Figure 9
Manual digitisation, ice patch (0.06 km ²)	Digervarden	S2, O	A of ice patches was 38% larger than S2. S2 mapping did not capture all parts of small bodies with dark surfaces	4.5.3 Figure 10
Manual digitisation (2 dig), Langfonna (0.4 km ²) and lakes	Langfonna, Hardangerjøkulen	S2, O	Langfonna: S2 glacier A was 4–7% larger than O and lake A 0.2–1.2% larger (S2 date 12 days earlier). Hardanger: S2 area of 4 lakes was both smaller and larger than O	4.5.4 Table 2 Figure 11
Manual digitisation, 2 ice caps (36 and 6.4 km ²)	Øksfjordjøkelen, Langfjordjøkelen	S2, P	S2 A was 1.2% (Ø) and 3.1% (L) larger than P	4.5.5
Comparison of two independent mapping approaches	Troms and Finnmark	S2, L8	S-2 area was 6% smaller than L8 for ~200 glaciers. For four ice caps glacier A was 3.3% smaller than L8 (S2 date 42 days later)	6.2 Table 5 Figure 12, 18
Applying buffer of ±5, ±10 m around glacier outlines	Norway and a selection of glacier samples and sizes	S2	All of Norway: ±3.1%, ±6% change in total A. Larger (smaller) sensitivity in relative A difference for smaller (larger) glaciers	6.3 Table 6 Figure 19

A, area; S2, Sentinel-2; L8, Landsat-8; O, aerial orthophoto; P, Pleiades satellite orthoimage. All S2 areas refer to the final edited result unless noted. One digitisation per object unless noted (2 dig) in first column. See Figure 1 for location of the glaciers.

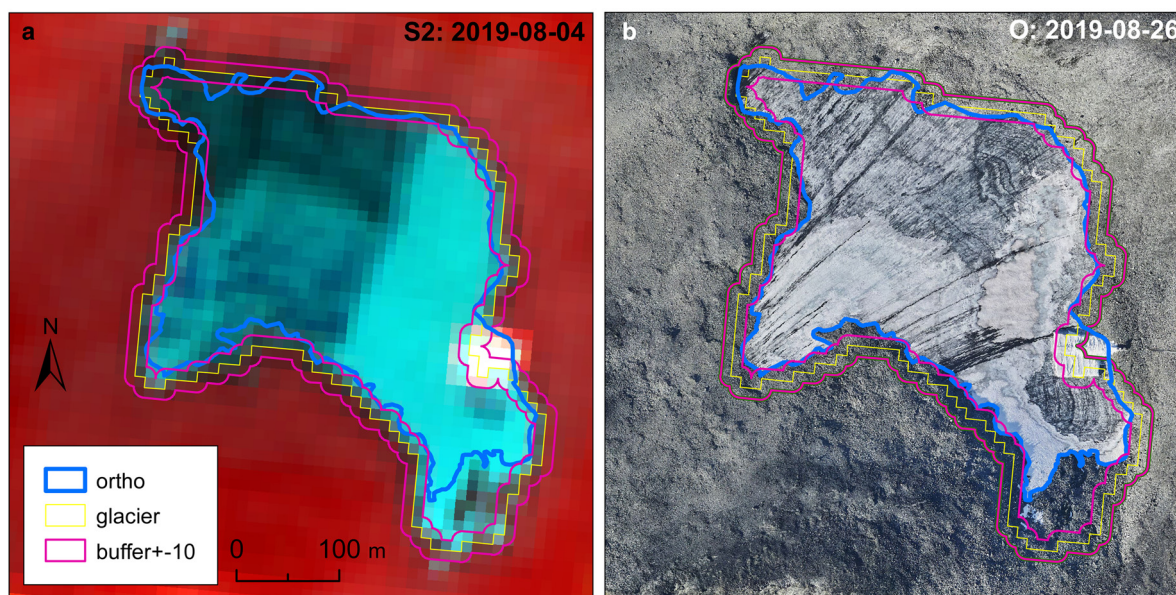


Fig. 19. Effect of a ±10 m buffer around the glacier polygons on the total area extent of Juvfonne with (a) Sentinel-2 image of 4 August 2019 in the background and (b) orthophoto of 26 August 2019 in the background. Ortho, outline manually digitised from orthophoto; glacier, automatically mapped from Sentinel-2. See Table 6. /Copernicus Sentinel data 2019/orthophoto Terratec/NVE/.

Our work demonstrated that it was easier to find scenes from Sentinel-2 than from Landsat used in the previous inventories due to the higher temporal resolution of Sentinel-2. We were able to cover all of mainland Norway over two subsequent years, 2018–2019, whereas the previous 1999–2006 inventory used scenes from a 7-year period. Using Sentinel-2 or Landsat-8 images from earlier in the melt season led to an overestimation of the glacier area due to more seasonal snow. However, early scenes were useful to check parts in shadow due to less terrain-induced shadowing. The higher spatial resolution of Sentinel-2 made it easier to identify

smaller glaciers and lakes than in the previous glacier and glacier lake inventories. Orthophotos are a good supplement for training, validation and classification and can be used to create inventories in smaller regions. Deriving glacier and glacier lake outlines from orthophotos for all of mainland Norway over a short time interval is not yet possible with the data available at norgebilder.no. The orthophotos span a too long period and many of them have adverse snow conditions. Using Sentinel-2 images and applying the standard semi-automated method with band ratio and manually selecting thresholds mapped clean ice accurately. Careful inspection of

all bodies and manual corrections were however needed. Manual inspection is time consuming and prone to errors. Differences in human interpretation or difficult mapping conditions due to snow, debris or clouds still cause uncertainties and inhomogeneities in the result. For the glacier lake mapping, we used both NDWI calculations and manual digitisation. We found that the accuracy in the semi-automatic mapping used here is as accurate or better than automatic approaches using NDWI and can be faster for a region of the size of mainland Norway.

Supplementary material. The supplementary material for this article can be found at <https://doi.org/10.1017/jog.2022.20>.

Data. The previous glacier outlines and glacier lake outlines are available at <https://nve.brage.unit.no/nve-xmlui/handle/11250/2830933> as part of the CryoClim collection. The new 2018–19 glacier outlines and lake outlines are available at: <https://nve.brage.unit.no/nve-xmlui/handle/11250/2828121> as part of the Copernicus glacier service collection. The glacier and glacier lake outlines are submitted to GLIMS <https://www.glims.org/>. We there included a few glacier outlines on the border between Norway and Sweden. The Swedish parts of the glaciers are not included in the glacier area of Norway.

Acknowledgements. We thank editor Fanny Brun and associate chief editor Nicolas Cullen for handling the manuscript and reviewer Frank Paul and one anonymous reviewer for numerous comments that improved the manuscript. This work is a contribution to the project Copernicus brejteneste (Copernicus Glacier Service Norway, Contract NIT.06.15.5/NIT.08.19.5) and to the JOSTICE, CryoClim and FonnSat projects. We thank Solveig H. Winsvold (NVE) for work on the Copernicus project and for making processing scripts available. We thank the European Space Agency for providing freely available Sentinel-2 imagery and for providing orthorectified imagery using the Norwegian DTM. We thank Etienne Berthier (LEGOS) and Centre National d'Etudes Spatiales (CNES) for providing Pléiades orthophotos. We thank Ivar Peerebom (NVE) for geodatabase design and updates of NVE's digital glacier atlas. Paul Weber digitised the Pléiades outline of Øksfjordjøkelen. Chris Stokes (Durham University), Rune Engeset (NVE) and Hallgeir Elvehøy (NVE) provided valuable comments to the manuscript. George Stanley Cowie provided language corrections and valuable comments.

Author contribution. T.N. selected, downloaded and processed the satellite images. L.M.A. and T.N. edited the glacier and glacier lake outlines and prepared the glacier and glacier lake 2018–19 datasets for southern and northern Norway, respectively. L.M.A. prepared the final datasets, created figures and tables, analysed results and wrote the text with contributions from T.N., B.K. and J.R.L. All authors digitised glacier outlines for validation and read and commented on the manuscript.

References

- Andreassen LM (ed.) and 5 others** (2021) Monitoring glaciers in mainland Norway and Svalbard using Sentinel. *NVE Rapport* 3–2021. Norwegian Water Resources and Energy Directorate, Oslo, Norway.
- Andreassen LM (ed.), Callanan M, Saloranta T, Kjølmoen B and Nagy T** (2020a) FonnSat – Fønner, arkeologi og satellittdata. *NVE Rapport* 41–2020. Norwegian Water Resources and Energy Directorate, Oslo, Norway.
- Andreassen LM, Elvehøy H, Kjølmoen B and Belart JMC** (2020b) Glacier change in Norway since the 1960s – an overview of mass balance, area, length and surface elevation changes. *Journal of Glaciology* **66**(256), 313–328. doi: [10.1017/jog.2020.10](https://doi.org/10.1017/jog.2020.10)
- Andreassen LM, Paul F, Kääb A and Hausberg JE** (2008) Landsat derived glacier inventory for Jotunheimen, Norway, and deduced glacier changes since the 1930s. *The Cryosphere* **2**, 131–145. doi: [10.5194/tc-2-131-2008](https://doi.org/10.5194/tc-2-131-2008)
- Andreassen LM and Winsvold SH** (2013) Algorithm Theoretical Basis Document (ATBD) for the GAO and GLO products. CryoClim sub-service for glaciers in mainland Norway. ESA/NSC PRODEX/Norway, CryoClim <https://hdl.handle.net/11250/2837094>.
- Andreassen LM, Winsvold SH, Paul F and Hausberg JE** (2012) Inventory of Norwegian Glaciers. *NVE report* 38–2012. Norwegian Water Resources and Energy Directorate, Oslo, Norway.
- Baumann S and 8 others** (2021) Updated inventory of glacier ice in New Zealand based on 2016 satellite imagery. *Journal of Glaciology* **67**(261), 13–26. doi: [10.1017/jog.2020.78](https://doi.org/10.1017/jog.2020.78)
- Bigelow DG and 5 others** (2020) The role of englacial hydrology in the filling and drainage of an ice-dammed lake, Kaskawulsh Glacier, Yukon, Canada. *Journal of Geophysical Research: Earth Surface* **125**, e2019JF005110. doi: [10.1029/2019JF005110](https://doi.org/10.1029/2019JF005110)
- Bogen J, Xu M and Kennie P** (2014) The impact of pro-glacial lakes on downstream sediment delivery in Norway. *Earth Surface Processes and Landforms* **40**, 942–952. doi: [10.1002/esp.3669](https://doi.org/10.1002/esp.3669)
- Bolch T, Buchroithner MF, Peters J, Baessler M and Bajracharya S** (2008) Identification of glacier motion and potentially dangerous glacial lakes in the Mt. Everest region/Nepal using spaceborne imagery. *Natural Hazards and Earth System Sciences* **8**, 1329–1340. doi: [10.5194/nhess-8-1329-2008](https://doi.org/10.5194/nhess-8-1329-2008)
- Bosson JB and Lambiel C** (2016) Internal structure and current evolution of very small debris-covered glacier systems located in alpine permafrost environments. *Frontiers in Earth Science* **4**, 39.
- Capps DM and Clague JJ** (2014) Evolution of glacier-dammed lakes through space and time; Brady Glacier, Alaska, USA. *Geomorphology*, **210**, 59–70. doi: [10.1016/j.geomorph.2013.12.018](https://doi.org/10.1016/j.geomorph.2013.12.018)
- Capt M, Bosson JB, Fischer M, Micheletti N and Lambiel C** (2016) Decadal evolution of a very small heavily debris-covered glacier in an Alpine permafrost environment. *Journal of Glaciology* **62**(233), 535–551.
- Carrivick JL and Tweed FS** (2013) Proglacial lakes: character, behaviour and geological importance. *Quaternary Science Reviews* **78**, 34–52. doi: [10.1016/j.quascirev.2013.07.028](https://doi.org/10.1016/j.quascirev.2013.07.028)
- Cogley JG and 10 others** (2011) Glossary of glacier mass balance and related terms. IHP-VII *Technical Documents in Hydrology No. 86*, IACS Contribution No. 2, Paris, UNESCO-IHP, 114.
- De Marco J and 6 others** (2020) Minor imbalance of the lowermost Italian glacier from 2006 to 2019. *Water* **12**(9), 2503. doi: [10.3390/w12092503](https://doi.org/10.3390/w12092503)
- Etzelmüller B and Hagen JO** (2005) Glacier-permafrost interaction in Arctic and alpine mountain environments with examples from southern Norway and Svalbard. In Harris C and Murton JB (eds), *Cryospheric Systems: Glaciers and Permafrost*, vol. **242**. Geological Society, London, Special Publications, pp. 11–27.
- Finstad E, Martinsen J, Hole R and Pilø L** (2018) Prehistoric and Medieval skis from glaciers and ice patches in Norway. *Journal of Glacial Archaeology* **3**, 43–58. doi: [10.1558/jga.33147](https://doi.org/10.1558/jga.33147)
- Fischer M, Huss M, Barboux C and Hoelzle M** (2014) The New Swiss Glacier Inventory SGI2010: relevance of using high-resolution source data in areas dominated by very small glaciers. *Arctic Antarctic and Alpine Research* **46**, 933–945. doi: [10.1657/1938-4246-46.4.933](https://doi.org/10.1657/1938-4246-46.4.933)
- Gao B** (1996) NDWI – a normalized difference water index for remote sensing of vegetation liquid water from space. *Remote Sensing of Environment* **58**(3), 257–266. doi: [10.1016/S0034-4257\(96\)00067-3](https://doi.org/10.1016/S0034-4257(96)00067-3)
- Granshaw FD and Fountain AG** (2006) Glacier change (1958–1998) in the North Cascades National Park Complex, Washington, USA. *Journal of Glaciology* **52**, 251–256. doi: [10.3189/172756506781828782](https://doi.org/10.3189/172756506781828782)
- GTN-G** (2017) GTN-G glacier regions. Global Terrestrial Network for Glaciers. doi: [10.5904/gtng-glacreg-2017-07](https://doi.org/10.5904/gtng-glacreg-2017-07). Online access Available at <http://dx.doi.org/10.5904/gtng-glacreg-2017-07>.
- Hannesdóttir H and 8 others** (2021) A national glacier inventory and variations in glacier extent in Iceland from the Little Ice Age maximum to 2019. *Jökull* **70**, 1–34. doi: [10.33799/jokull2020.70.111](https://doi.org/10.33799/jokull2020.70.111)
- Harrison S and 14 others** (2018) Climate change and the global pattern of moraine-dammed glacial lake outburst floods. *The Cryosphere* **12**, 1195–1209. doi: [10.5194/tc-12-1195-2018](https://doi.org/10.5194/tc-12-1195-2018)
- Helfricht K, Lehning M, Sailer R and Kuhn M** (2015) Local extremes in the lidar-derived snow cover of alpine glaciers. *Geografiska Annaler: Series A, Physical Geography* **97**(4), 721–736.
- How P and 10 others** (2021) Greenland-wide inventory of ice marginal lakes using a multi-method approach. *Scientific Reports* **11**(4481), 1–13. doi: [10.1038/s41598-021-83509-1](https://doi.org/10.1038/s41598-021-83509-1)
- Kääb A and 5 others** (2016) Glacier remote sensing using Sentinel-2. Part I: radiometric and geometric performance, and application to ice velocity. *Remote Sensing* **8**(7), 598.
- Kjølmoen B (Ed.), Andreassen LM, Elvehøy H and Melvold K** (2021) Glaciological investigations in Norway 2020. NVE Rapport 31–2021. Norwegian Water Resources and Energy Directorate, Oslo, Norway.
- Leigh JR and 5 others** (2019) Identifying and mapping very small (<0.5 km²) mountain glaciers on coarse to high-resolution imagery. *Journal of Glaciology* **65**(254), 873–888. doi: [10.1017/jog.2019.50](https://doi.org/10.1017/jog.2019.50)
- Leigh JR, Stokes CR, Evans DJA, Carr JR and Andreassen LM** (2020) Timing of ‘Little Ice Age’ maxima and subsequent glacier retreat in

- northern Troms and western Finnmark, northern Norway. *Arctic Antarctic, and Alpine Research* 52(1), 281–311. doi: [10.1080/15230430.2020.1765520](https://doi.org/10.1080/15230430.2020.1765520)
- Liestøl O** (1956) Glacier dammed lakes in Norway. *Norsk Geografisk Tidsskrift, Bind* 15, Oslo, 122–149.
- Liestøl O** (1962) List of the area and number of glaciers. In A. Hoel and W. Werenskiold, eds. *Glaciers and snowfields in Norway*. Norsk Polarinstitutt Skrifter, 114, 35–54.
- Linsbauer A and 7 others** (2021) The New Swiss Glacier Inventory SGI2016: from a topographical to a glaciological dataset. *Frontiers in Earth Science* 9, 1–22. doi: [10.3389/feart.2021.704189](https://doi.org/10.3389/feart.2021.704189).
- Matta E, Giardino C, Boggero A and Bresciani M** (2017) Use of satellite and in situ reflectance data for lake water color characterization in the Everest Himalayan region. *Mountain Research and Development* 37(1), 16–23. doi: [10.1659/MRD-JOURNAL-D-15-00052.1](https://doi.org/10.1659/MRD-JOURNAL-D-15-00052.1)
- Meier WJH, Griesinger J, Hochreuther P and Braun MH** (2018) An updated multi-temporal glacier inventory for the Patagonian Andes with changes between the Little Ice Age and 2016. *Frontiers in Earth Science* 6, 62. doi: [10.3389/feart.2018.00062](https://doi.org/10.3389/feart.2018.00062)
- Nagy T and Andreassen LM** (2019) Glacier lake mapping with Sentinel-2 imagery in Norway. *NVE Rapport* 40–2019. Norwegian Water Resources and Energy Directorate, Oslo, Norway.
- Nesje A and 9 others** (2012) The climatic significance of artefacts related to prehistoric reindeer hunting exposed at melting ice patches in southern Norway. *The Holocene* 22, 485–496.
- Ødegård RS and 6 others** (2017) Climate change threatens archaeologically significant ice patches: insights into their age, internal structure, mass balance and climate sensitivity. *The Cryosphere* 11, 17–32. doi: [10.5194/tc-11-17-2017](https://doi.org/10.5194/tc-11-17-2017)
- Olson M and Rupper S** (2019) Impacts of topographic shading on direct solar radiation for valley glaciers in complex topography. *The Cryosphere* 13, 29–40. doi: [10.5194/tc-13-29-2019](https://doi.org/10.5194/tc-13-29-2019)
- Østrem G, Dale Selvig K and Tandberg K** (1988) Atlas over breer i Sør-Norge (Atlas of glaciers in South Norway), Hydrologisk avdeling, Norges Vassdrags- og Energiverk. *Meddelelse* 61, 180.
- Østrem G, Haakensen N and Melander O** (1973) Atlas over breer i Nord-Skandinavia (Glacier atlas of Northern Scandinavia), Hydrologisk avdeling, Norges Vassdrags- og Energiverk. *Meddelelse* 22, 315.
- Østrem G and Ziegler T** (1969) Atlas over breer i Sør-Norge (Atlas of glaciers in South Norway), Hydrologisk avdeling, Norges Vassdrags- og Elektrisitetsvesen. *Meddelelse* 20, 207.
- Paul F and 9 others** (2009) Recommendations for the compilation of glacier inventory data from digital sources. *Annals of Glaciology* 50(53), 119–126. doi: [10.3189/172756410790595778](https://doi.org/10.3189/172756410790595778)
- Paul F and 19 others** (2013) On the accuracy of glacier outlines derived from remote-sensing data. *Annals of Glaciology* 54, 171–182.
- Paul F and 10 others** (2020) Glacier shrinkage in the Alps continues unabated as revealed by a new glacier inventory from Sentinel-2. *Earth System Science Data* 12, 1805–1821. doi: [10.5194/essd-12-1805-2020](https://doi.org/10.5194/essd-12-1805-2020)
- Paul F and Andreassen LM** (2009) A new glacier inventory for the Svartisen region (Norway) from Landsat ETM+ data: challenges and change assessment. *Journal of Glaciology* 55(192), 607–618.
- Paul F, Frey H and Le Bris R** (2011) A new glacier inventory for the European Alps from Landsat TM scenes of 2003: challenges and results. *Annals of Glaciology* 52(59), 144–152. doi: [10.3189/172756411799096295](https://doi.org/10.3189/172756411799096295)
- Paul F and Kääb A** (2005) Perspectives on the production of a glacier inventory from multispectral satellite data in Arctic Canada: Cumberland Peninsula, Baffin Island. *Annals of Glaciology* 42, 59–66. doi: [10.3189/172756405781813087](https://doi.org/10.3189/172756405781813087)
- Paul F, Winsvold SH, Kääb A, Nagler T and Schwaizer G** (2016) Glacier remote sensing using Sentinel-2. Part II: mapping glacier extents and surface facies, and comparison to Landsat 8. *Remote Sensing* 8(7), 575.
- Pfeffer WT and 18 others** (2014) The Randolph Glacier Inventory: a globally complete inventory of glaciers. *Journal of Glaciology* 60(221), 537–552. doi: [10.3189/2014JG13J176](https://doi.org/10.3189/2014JG13J176)
- Pilo LH, Barrett JH and Eiken T** (2021) Interpreting archaeological site-formation processes at a mountain ice patch: a case study from Langfonne, Norway. *The Holocene* 31(3), 469–482. doi: [10.1177/0959683620972775](https://doi.org/10.1177/0959683620972775)
- Qayyum N, Ghuffar S, Ahmad HM, Yousaf A and Shahid I** (2020) Glacial lakes mapping using multi satellite PlanetScope imagery and deep learning. *ISPRS International Journal of Geo-Information* 9, 560. doi: [10.3390/ijgi9100560](https://doi.org/10.3390/ijgi9100560)
- Racoviteanu AE, Paul F, Raup B, Khalsa SJS and Armstrong R** (2009) Challenges and recommendations in mapping of glacier parameters from space: results of the 2008 Global Land Ice Measurements from Space (GLIMS) workshop, Boulder, Colorado, USA. *Annals of Glaciology* 50, 53–69.
- Raup BH and 11 others** (2007) Remote sensing and GIS technology in the Global Land Ice Measurements from Space (GLIMS) Project. *Computers and Geosciences* 33, 104–125.
- Raup B and Khalsa SJS** (2007) GLIMS analysis tutorial. National Snow and Ice Data Center, Boulder, CO. Available at <http://glims.org/MapsAndDocs/guides.html>.
- Reynolds JM** (1999) Glacial hazard assessment at Tsho Rolpa, Rolwaling, Central Nepal. *Quarterly Journal of Engineering Geology and Hydrogeology* 32, 209–214. doi: [10.1144/GSL.QJEG.1999.032.P3.01](https://doi.org/10.1144/GSL.QJEG.1999.032.P3.01)
- RGI Consortium** (2017) Randolph Glacier Inventory – a dataset of global glacier outlines: version 6.0: technical report, global land ice measurements from space, Colorado, USA. *Digital Media*, 71 pp. doi: [10.7265/N5-RGI-60](https://doi.org/10.7265/N5-RGI-60)
- Shugar DH and 5 others** (2020) Rapid worldwide growth of glacial lakes since 1990. *Nature Climate Change* 10, 939–945. doi: [10.1038/s41558-020-0855-4](https://doi.org/10.1038/s41558-020-0855-4)
- Stokes C, Andreassen LM, Champion MR and Corner GD** (2018) Widespread and accelerating glacier retreat on the Lyngen Peninsula, northern Norway, since their ‘Little Ice Age’ maximum. *Journal of Glaciology* 64(243), 100–118. doi: [10.1017/jog.2018.3](https://doi.org/10.1017/jog.2018.3)
- Strozzi T, Wiesmann A, Kääb A, Joshi S and Mool P** (2012) Glacial lake mapping with very high resolution satellite SAR data. *Natural Hazards and Earth System Sciences* 12, 2487–2498. doi: [10.5194/nhess-12-2487-2012](https://doi.org/10.5194/nhess-12-2487-2012)
- Veh G, Korup O, Roessner S and Walz A** (2018) Detecting Himalayan glacial lake outburst floods from Landsat time series. *Remote Sensing of Environment* 207, 84–97. doi: [10.1016/j.rse.2017.12.025](https://doi.org/10.1016/j.rse.2017.12.025)
- Wangchuk S and Bolch T** (2020) Mapping of glacial lakes using Sentinel-1 and Sentinel-2 data and a random forest classifier: strengths and challenges. *Science of Remote Sensing* 2, 100008. doi: [10.1016/j.srs.2020.100008](https://doi.org/10.1016/j.srs.2020.100008)
- Weber P, Andreassen LM, Boston CM, Lovell H and Kvarteig S** (2020) An ~1899 glacier inventory for Nordland, northern Norway, produced from historical maps. *Journal of Glaciology* 66(256), 259–277. doi: [10.1017/jog.2020.3](https://doi.org/10.1017/jog.2020.3)
- Weber P, Boston CM, Lowell H and Andreassen LM** (2019) Evolution of the Norwegian plateau icefield Hardangerjøkulen since the ‘Little Ice Age’. *The Holocene* 29(12), 1885–1905. doi: [10.1177/0959683619865601](https://doi.org/10.1177/0959683619865601)
- Winsvold SH, Andreassen LM and Kienholz C** (2014) Glacier area and length changes in Norway with repeat inventories. *The Cryosphere* 8, 1885–1903. doi: [10.5194/tc-8-1885-2014](https://doi.org/10.5194/tc-8-1885-2014)
- Zhang Mm, Chen F and Tian Bs** (2018) An automated method for glacial lake mapping in High Mountain Asia using Landsat 8 imagery. *Journal of Mountain Science* 15, 13–24. doi: [10.1007/s11629-017-4518-5](https://doi.org/10.1007/s11629-017-4518-5)
- Zheng G and 11 others** (2021) Increasing risk of glacial lake outburst floods from future Third Pole deglaciation. *Nature Climate Change* 11, 411–417. doi: [10.1038/s41558-021-01028-3](https://doi.org/10.1038/s41558-021-01028-3)